Chapter 10

Badlands and Gullying

Alan D. Howard

Introduction

Badlands have fascinated geomorphologists for the same reasons that they inhibit agricultural use: lack of vegetation, steep slopes, high drainage density, shallow to non-existent regolith, and rapid erosion rates. Badlands appear to offer in a miniature spatial scale and a shortened temporal scale many of the processes and landforms exhibited by more normal fluvial landscapes, including a variety of slope forms, bedrock or alluvium-floored rills and washes, and flat alluvial expanses similar to large-scale pediments. Although badlands evoke an arid image, they can develop in nearly any climate in soft sediments where vegetation is absent or disturbed. For example, short-lived badlands have been documented in the temperate climate of the eastern United States in sediment waste piles (Schumm 1956a) and borrow pits (Howard and Kerby 1983).

Gullies are closely related to badlands in that they record accelerated erosion into regolith or soft sediment by processes that are generally identical to those occurring in badlands. Large gully systems can evolve into badlands. Gullying occurs primarily in response to local disturbance of a vegetation cover by climate change, fire, or land-use changes and some badlands, such as the classic ones in South Dakota, have evolved through incision into a vegetated uplands.

This chapter will emphasize the relationship between process and form in badlands and gullied landscapes and their long-term evolution through both descriptive and quantitative modelling.

A.D. Howard (✉)
Department of Environmental Sciences, University of Virginia, Charlottesville, VA 22904-4123, USA
e-mail: ah6p@cms.mail.virginia.edu

Badlands

General reviews of badlands and badland processes are provided by Campbell (1989) and Bryan and Yair (1982a), including discussion of the climatic, geologic, and geographic setting of badlands, sediment yields, host rock and regolith variations among badlands, field measurements of processes.

Badland Regolith and Processes

The often (but not universally) rapid landform evolution in badlands provides the prospect of direct observational coupling of process and landform evolution in both natural and man-induced badlands. However, Campbell (1989) and Campbell and Honsaker (1982) caution about problems of scaling between processes on badland slopes and channels to larger landforms. Furthermore, although badland slopes commonly exhibit smooth profiles and areally uniform surface texture, (Figs. 10.1 and 10.2), recent studies have demonstrated that weathering, mass-wasting, and water erosional processes on badland slopes exhibit complex spatial and temporal variability and that weathering and erosional processes are largely hidden from direct observation in cracks and micropipes (Bryan et al. 1978, Yair et al. 1980, Bouma and Imeson 2000, Kuhn and Yair 2004, Kasanin-Grubin and Bryan 2007).

A.J. Parsons, A.D. Abrahams (eds.), *Geomorphology of Desert Environments*, 2nd ed.,
DOI 10.1007/978-1-4020-5719-9_10,

Fig. 10.1 Badlands in Mancos Shale near Caineville, Utah. *Top* of North Caineville Mesa in background is 360 m above alluvial surface in middle distance, and is capped by the 60 m thick Emery Sandstone. Note the sharp-crested, straight-sloped badlands in Mancos Shale in the middle distance which rise abruptly 30–50 m above the Holocene alluvial surface. Level ridge crests marked by '∗' are remnants of the Early Wisconsin (Bull Lake) pediment (photo by A. Howard)

Fig. 10.2 Rounded badland slopes in Morrison Formation near Hanksville, Utah (photo by A. Howard)

An Example: Badlands in the Henry Mountains Area, Utah

Shales of Jurassic and Cretaceous age exposed in the vicinity of the Henry Mountains, Utah, have in places been sculpted into dramatic badlands. The climate in the desert areas at about 1500 m above M.S.L. is arid, with about 125 mm of annual precipitation, most of which occurs as summer thunderstorms. These badlands provide premier examples of the erosional conditions favouring badlands, badland slope form and process, relationship between fluvial and slope processes, and variations of badland form with rock type. In particular, the great thickness and uniform lithology of the Upper Cretaceous Mancos Shale (Hunt 1953) results in an unusual spatial uniformity of slope form and process (Figs. 10.1 and 10.2), first described by Gilbert (1880). Badlands developed in this area on the Mancos Shale, the Morrison Formation, and the Summerville Formation will be used here as examples. These badlands are discussed more fully by Howard (1970, 1997).

Badland Regolith

Badlands generally have very thin regoliths in arid regions, ranging from about 30 cm to essentially unweathered bedrock. Many badland areas share a similar regolith profile. The top 1–5 cm is a surface layer exhibiting dessication cracks when dry. This surface layer is a compact crust with narrow polygonal cracking in the case of shales with modest shrink-swell (<25%) behavior, such as the Mancos Shale badlands in Utah (Fig. 10.3), the Brule Formation badlands in South Dakota (Schumm 1956a,b), and portions of the Dinosaur Badlands, Canada (Bryan et al. 1978, 1984, Hodges and Bryan 1982). With higher shrink-swell behaviour the surface layer is broken into irregular, loose 'popcorn' fragments with large intervening voids, as exemplified in badlands on the Chadron Formation in South Dakota, the Morrison (Fig. 10.4) and Chinle Formations in Utah, and portions of the Dinosaur Badlands, Canada. The surface layer may be thicker (10 or more centimeters) in such cases. Although the surface layer may contain a few partially weathered fragments of shale, vein fillings, nodules, etc., it is primarily composed of disaggregated and remolded shale, silt and sand weathered from the shale which is leached of highly soluble components (particularly when derived from marine shales such as the Mancos Shale (Laronne 1982).

Beneath the surface layer is a sublayer (crust) averaging about 5–10 cm in thickness which may range from a dense, amorphous crust (Hodges and Bryan 1982, Gerits et al. 1987) to a loose, granular layer (Howard 1970, Schumm and Lusby 1963). Part of the apparent variability of surface layer and crust may be due to differences among researchers in locating the division between these units. Below the crust there occurs a transitional 'shard layer' ranging from 10 to 40 cm in thickness consisting of partially disaggregated and weathered shale chips grading to firm, unweathered shale.

Fig. 10.3 Regolith profile in Mancos Shale badlands. Note smooth, mud-cracked surface crust, shard layer, and essentially unweathered shale at depth of about 15 cm. This is a marine shale dominated by Illite clay mineralogy. Note watch for scale (photo by A. Howard)

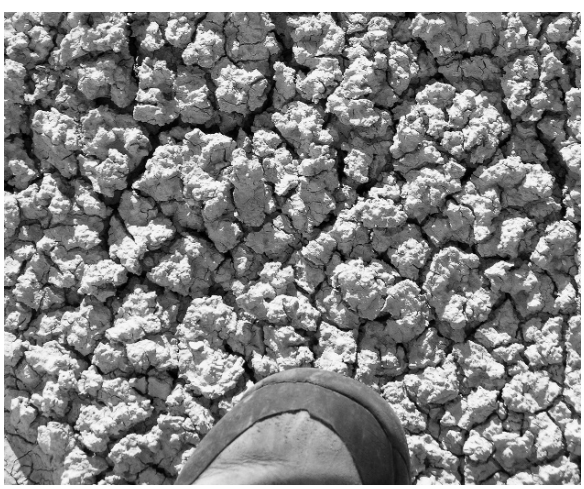

Fig. 10.4 Popcorn surface crust on Morrison Formation shale. Clays in these badlands are dominated by Smectite (Montmorillonite) clays with high shrink-swell potential (photo by A. Howard)

However, there is considerable variability in badland regoliths. Well-cemented sandstone layers outcrop as bare rock, often creating ledges or caprocks. Slightly cemented sand layers (often with $CaCO_3$ cement) generally form steep slopes with regolith 1–5 mm thick or less (Gerits et al. 1987, Hodges and Bryan 1982, Bowyer-Bower and Bryan 1986). These sandstones may develop permanent rill networks (Kasanin-Grubin and Bryan 2007). Carman (1958) described a regolith in fluted badlands in a clay matrix-supported conglomerate composed of a hard veneer of sandy clay 10–15 cm thick over a softer interior layer and a hard core. Badlands on shaly sandstones in the Summerville Formation have a non-cohesive surface layer of sand grains and shale chips which grades fairly uniformly to unweathered bedrock within 10–20 cm. Some badland surfaces are cemented with a biological crust of algae or lichens (Yair et al. 1980, Finlayson et al. 1987). In badlands where the shale has non-dispersive clays or physical weathering processes dominate, surface crusts may be absent, with a thin shard layer grading to solid shale within a few centimetres (Figs. 10.5 and 10.6). Badlands in marine shales, such as the Mancos Shale, may have salt recrystallization in the sublayers and local areas of salt surface crusts (Laronne 1982). Due to the frequent occurrence of rapid mass wasting on steep badland slopes, recently denuded areas have atypically thin regoliths with poor development of the surface layer.

Systematic variations in regolith properties may be associated with slope aspect. Churchill (1981), in

Fig. 10.5 Badlands near Lumbier, Navarra, Spain. Note rounded divides and linear lower slope profiles. (Photo by A. Howard)

Fig. 10.6 Surface texture of badlands shown in Fig. 10.5. Regolith consists primary of shards up to 1 cm in size with unaltered bedrock within a few centimeters (photo by A. Howard)

a comparison of north- and south-facing slopes in Brule Formation Badlands (South Dakota), found the north-facing slopes to be more gently sloping, more densely rilled, with deeper regoliths, and characterized by infrequent mass-wasting involving much of the regolith (20–30 cm). By contrast, south-facing slopes have frequent shallow (3–10 cm thick) sloughing failures. Churchill suggested that slower evaporation promotes deeper infiltration on north-facing slopes. Yair et al. (1980) and Kuhn and Yair (2004) found that north-facing slopes in the Zin badlands of the Negev desert to have a rough, lichen-covered surface, a deeper regolith, few rills, and relatively high runoff and erosion. South-facing slopes are smoother, with greater runoff, frequent mudflows, and pipe development, but they experience less runoff erosion overall.

Weathering processes of badland regolith development involve relatively modest changes in mineralogy, since the source rocks are poorly lithified sedimentary rocks. Simple wetting may be sufficient to disaggregate the shale and disperse the clay minerals. For example, unweathered blocks of Morrison Formation smectitic shales will completely disaggregate and disperse within a few minutes to a few hours in just enough water to completely saturate the sample (this may be a considerable relative volume of water because of the pronounced swelling). Rapid slaking accompanies this disaggregation. The shallow regolith on these slopes testifies to the absorptive capacity and impermeability of the surface layers. On the other hand, samples of unweathered Mancos Shale, a marine shale in which illite is dominant, decompose more slowly, with less swelling and incomplete dispersion. A yellowish liquor of dissolved salts (mostly sodium and calcium sulfates: Laronne 1981, 1982) is produced, the accumulation of which apparently inhibits further disintegration. Leaching of these solutes is apparently required for complete weathering, and salt concentrations decrease upwards within the regolith (Laronne 1982). Some clayey sandstones may have a calcite cementing which requires dissolution before erosion, and the regolith is only a few millimeters thick (Bowyer-Bower and Bryan 1986). On the other hand, marls composed of more than 50% calcite and gypsum may be essentially free from cementation. Consequently clay mineral dispersion is all that is required to form a disaggregated regolith (Finlayson et al. 1987, Imeson and Verstraten 1985). Some unconsolidated sediments require no weathering prior to entrainment by rainsplash and runoff, so that regolith is absent or only seasonally present due to frost heaving (for example, the artificial Perth Amboy badlands of Schumm 1956a).

The structure and appearance of badland regolith may change appreciably in response to the sequence of precipitation events. Kasanin-Grubin and Bryan (2007) document a change in surface texture over two years on badlands in Alberta, Canada from an open, popcorn surface (similar to Fig. 10.4) to a dense, cracked crust (similar to Fig. 10.3) over a two year period in response to snowfalls and low intensity, long-duration rainfall. They also conducted experiments demonstrating that low duration rainstorms produce popcorn textures through shrinkage and swelling while long-duration rainstorms produce coherent crusts through clay dispersion. Greater runoff and deeper rill erosion accompany the formation of coherent crusts.

The physical and chemical properties of clay minerals, grain size distribution, density, and cementation affect the weathering by wetting and leaching, runoff characteristics, sediment and solute yields, and badland form. The properties of shales relevant to their erosional behaviour can be measured by a number of simple physico-chemical tests of cation-exchange capacity, solute extracts (concentration and chemistry), Atterberg (consistency) limits, vane shear strength, dispersion index, aggregate stability, shrink-swell behavior (Imeson et al. 1982, Imeson and Verstraten 1988, Hodges and Bryan 1982, Bryan et al. 1984, Gerits et al. 1987, Bouma and Imeson, 2000, Faulkner et al., 2000, 2003).

Erosional Processes on Badland Slopes

Discussion of slope erosional processes is conventionally divided into mass-wasting (creep, sliding, and flowage) and wash processes (runoff and rainsplash erosion). This discussion follows that division, although these processes are so interrelated and intergrading that such divisions are primarily for convenience.

Mass-Wasting

The rounded slopes of the Morrison (Fig. 10.2), Chinle, and Chadron formations have been attributed to the dominance of creep as a slope-forming process (Davis 1892, Schumm 1956b, Howard 1970). These formations contain clays with high dispersive and shrink-swell potential. The volume changes occurring during wetting together with the loss of bulk strength encourage downslope sag and creep of surface layers. Schumm (1963) found surface creep rates to be proportional to the sine of the slope gradient for slope gradients less than 40° on Mancos Shale, and such a relationship is likely to be a good approximation to mass-wasting rates for low slope gradients.

Many badland sideslopes are close to their maximum angle of stability, as long, narrow, shallow slips are common occurrences. Because these slopes are generally at angles of 40° or more, and failures occur during rainstorms, slope stability can be analyzed by the well known infinite slope model for saturated regolith and flow parallel to the slope (e.g., Lambe and Whitman 1969, pp. 352–356, Carson 1969, p. 87, Carson and Kirkby 1972, pp. 152–159). Figure 10.7 shows the definitions for an analysis similar to Lambe and Whitman's except that uniform surface flow is also allowed. Conditions for failure at a depth d_r below the surface are assumed to be approximated by a linear relationship:

$$\tau_f = c + \sigma_e \tan\varphi, \tag{10.1}$$

where τ_f is the shear stress on the failure plane, σ_e is the effective normal stress on the failure plane, c is the saturated cohesion, and ϕ is the saturated friction angle for the regolith material.

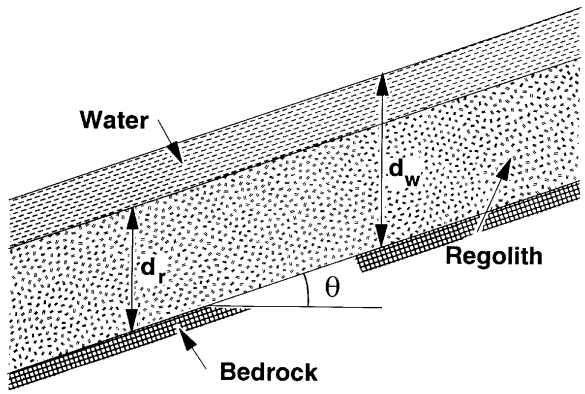

Fig. 10.7 Definition of terms for infinite slope failure with water flowing parallel to the slope surface

Based upon Fig. 10.3 for the case when $d_w \geq d_r$ the shear and effective normal stresses on the potential failure plane are:

$$\sigma_e = \rho_b \, d_r \, g \cos^2\theta \tag{10.2}$$

and

$$\tau = \left[\rho_t \, d_r + \rho_w (d_w - d_r)\right] g \sin\theta \cos\theta \tag{10.3}$$

where ρ_b and ρ_t are the buoyant and total densities of the regolith, respectively, ρ_w is the water density, g is the gravitational constant, θ is the slope angle, and d_w is the depth of water flow above the regolith surface. For the case when $d_w < d_r$

$$\sigma_e = \left[\rho_u (d_r - d_w) + \rho_b \, d_w\right] g \cos^2\theta \tag{10.4}$$

and

$$\tau = \left[\rho_u (d_r - d_w) + \rho_t \, d_w\right] g \sin\theta \cos\theta \tag{10.5}$$

where ρ_u is the unsaturated unit weight of the regolith (which is likely to be very close to ρ_t).

Failure occurs when $\tau \geq \tau_f$. For the shallow badland regoliths only slight cohesion is necessary to permit slopes greater than 40° if water flow depths are small. For typical values of regolith density complete saturation with flow parallel to the surface reduces maximum slope angles by a factor of about two (Lambe and Whitman, 1969). Under such conditions badland slopes may fail as mudflows (Yair et al. 1980, Battaglia et al. 2002, Kuhn and Yair 2004, Desir and Marín 2006, Nadal-Romero et al., 2007).

Wash Processes

Wash processes on badlands occur only during and immediately after rainstorms. If a rainstorm starts with a dry regolith (the usual case) much of the initial rainfall is absorbed by the regolith and initially penetrates deeply along cracks and between popcorn aggregates, if present. Runoff from badland slopes is delayed for several minutes after rainfall initiates; for example, Bryan et al. (1984) note a delay of 10–15 min after initiation of sprinkling at a rate of 10–20 mm h^{-1}. The depth of wetting is limited either by absorption along crack and fissure edges or by ponding on top of the dense crust layer, if present (Hodges and Bryan 1982). Swelling of the regolith clays rapidly begins to close the cracks and gaps, so that flow is increasingly restricted to lateral flow in larger cracks and, in many cases to micropipes developed near the crust-shard layer boundary (Hodges and Bryan 1982) (Fig. 10.8). The flow in the larger cracks which receive appreciable flow from upslope may be able to erode their walls and keep pace with regolith swelling (Engelen 1973). Most of these will be ephemeral rills, which are partly or wholly eradicated by continued swelling

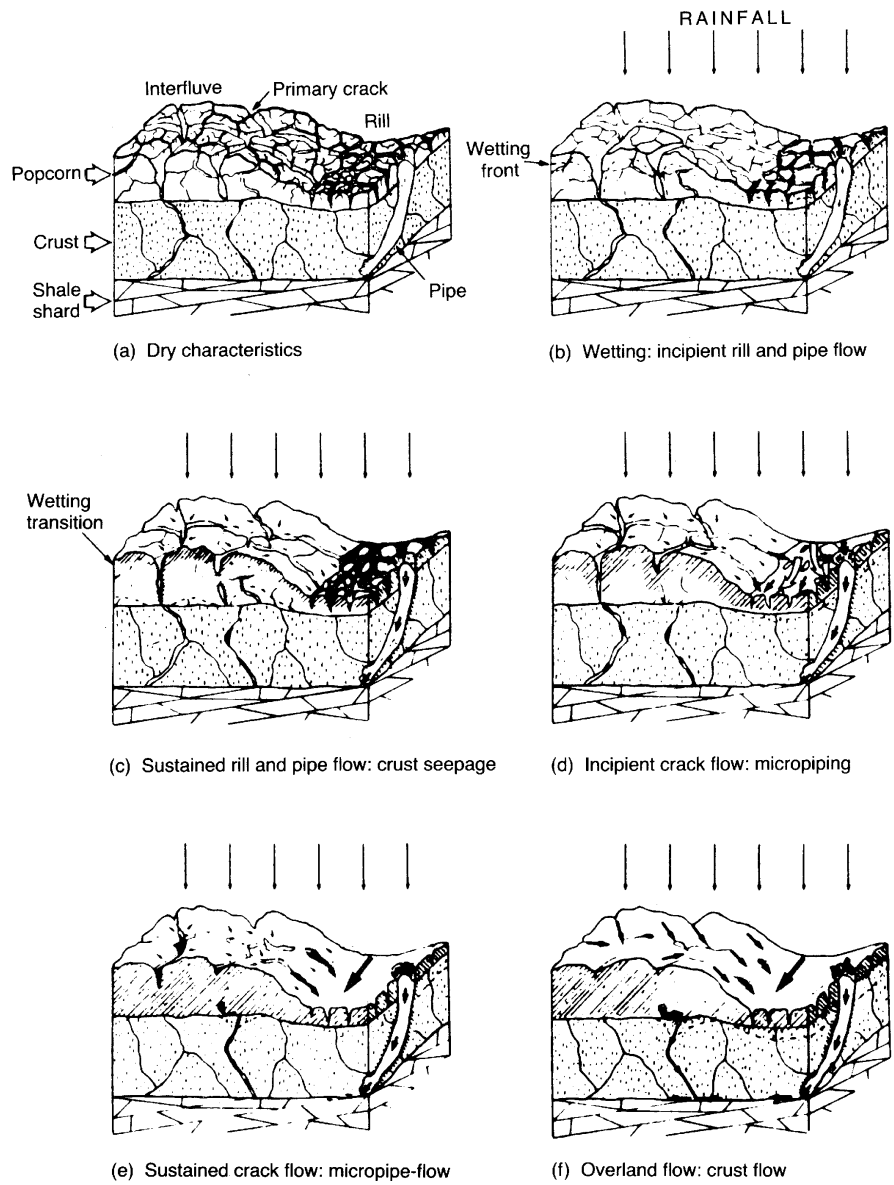

Fig. 10.8 Regolith structure and runoff behavior on shale badland slopes. Diagrams (**a**–**f**) portray successive stages in wetting and runoff development. (from Hodges and Bryan 1982, Fig. 2.7)

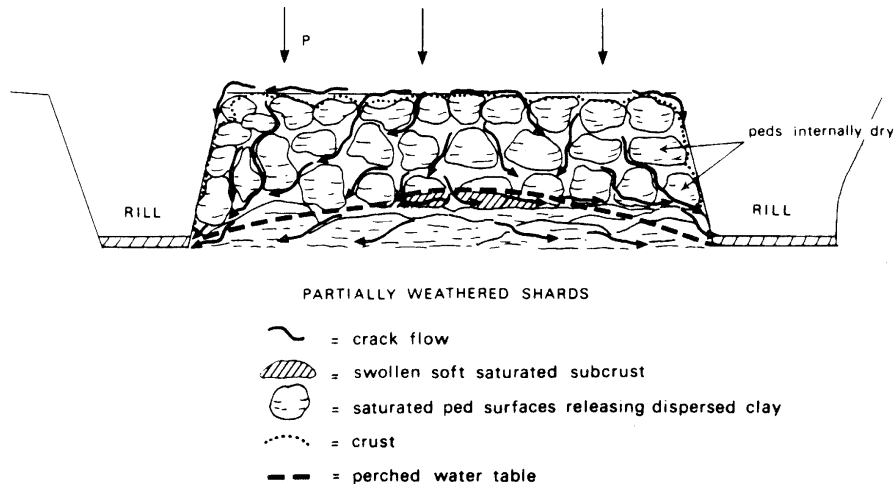

Fig. 10.9 Development of a perched water table on top of shard layer in badland regolith and lateral drainage to rills. Note development of a saturated, soft layer between the rills which may fail, forming a pipe and eventually a new rill. (from Imeson and Verstraten 1988, Fig. 10.1)

and subsequent drying and cracking of the surface layer. Sediment is added to the flow both by shear and dispersion of clay minerals, and the sediment load may range up to mudflow concentrations. Flow in the cracks and micropipes eventually feeds into rills or onto alluvial surfaces. Badland interflow has been compared to intergranular flow to drains (the rills) (Gerits et al. 1987, Imeson and Verstraten 1988) (Fig. 10.9). Surface rills may initiate through liquefaction of saturated, dispersed crust above the shard layer with accompanying runout, pipe formation and surface collapse in the zones of greatest depth of saturation between surface rills (Fig. 10.9).

Hodges and Bryan (1982) pointed out that in Dinosaur Badlands, Canada, runoff occurs more rapidly and more completely on silty surfaces which locally encrust badland rills than on the cracked surface layers of badland slopes. Such silty layers in rills are uncommon on badlands in the Henry Mountains region, but alluvial surfaces are generally covered by such sediment and have rapid runoff response. Cerdà and García Fayos (1997) also note more complete runoff from alluvial surfaces than badland slopes. A few very gentle badland slopes in Morrison Shale exhibit a banding alternating between typical popcorn-textured badland slopes and short alluvial surfaces (Fig. 10.10). The absence of shrink-swell cracking of the alluvial surfaces suggests that the silt layers are very effective at preventing infiltration. The banding may be an expression of layering in the shale or it may indicate a natural bifurcation at low slope gradient between normal badland slopes with swelling enhanced by water shed from upslope alluvial patches and alluvial surfaces graded downstream to the swollen shale bands.

Fig. 10.10 Low, terraced hillslope on shale in Morrison Formation. White bands are small segments of alluvial surface (photo by A. Howard)

In some badlands much of the slope drainage is routed through deep, corrasional pipe networks (see reviews in Campbell 1989, Harvey 1982, Jones 1990, Parker et al. 1990, several papers in Bryan and Yair 1982b, Faulkner et al. 2007). Piping in susceptible lithologies is encouraged by prominent jointing and steeper hydraulic gradients via underground rather than surface paths caused by layering in the bedrock or though dissection of an originally flat upland (Campbell 1989). Faulkner et al. (2007) discuss a badlands landscape in which the initial response to downcutting by the master drainage is development of a deep piping network which then, through collapse, forms an integrated surface network of channels. Piping is rare in the Henry Mountains badlands discussed here.

Rainsplash

Rainsplash erosion is important on badlands both as a direct agent of detachment and splash transport and indirectly as detachment contributes to runoff erosion and affects the flow hydraulics of shallow flows. A considerable experimental literature exists on rainsplash erosion mechanics (see Chapter 9); the major controlling variables are raindrop size and velocity, rain intensity, and regolith characteristics. Few direct measurements exist of the contribution of rainsplash to badland slope erosion. Howard (1970) and Moseley (1973) attributed narrow, rounded divides on some badlands to the action of rainsplash rather than creep, and the rounded slopes with very thin regolith on the badlands in Fig. 10.5 may be due to diffusive rainsplash erosion. Carson and Kirkby (1972, p. 221) also suggest divide convexity may be caused by rainsplash on some arid slopes. The influence of rainsplash may be limited at the beginning of rainstorms by the cohesiveness of the dry clay, and biotic crusts, where present, protect shale regolith from rainsplash entrainment (Yair et al. 1980, Finlayson et al. 1987). In contrast to rock-mantled slopes, rainsplash has modest direct influence on overland flow hydraulics due to the concentration of flow into cracks and micropipes.

Runoff Erosion

Runoff on badlands seldom exemplifies the classic characteristics of overland flow on agricultural land because of the concentration of flow into cracks, micropipes, and ephemeral rills. The rate of erosion in such channelled overland- and inter-flow, as well as in larger rills and washes functionally depends upon flow conditions and resistance of the bedrock or regolith to weathering or detachment. The processes of erosion are poorly understood but may involve direct detachment from the bedrock, scour by sediment, and weathering processes such as leaching and wetting with dispersion.

Several approaches have been used to quantify runoff erosion in both rills and interrill areas. The most common approach on agricultural slopes is to estimate sediment transport rates using bedload or total load transport formulas assuming that the flow is loaded to capacity in the sand size ranges (transport-limited conditions). These are often empirically corrected for rainsplash effects based upon results of plot experiments in non-cohesive sediments or weakly cohesive soils (e.g. Meyer and Monke 1965, Komura 1976, Gilley et al. 1985, Julian and Simons 1985, Everaert 1991, Kinnell 1990, 1991). Detachment by rainsplash is assumed to assure capacity transport even where soils are moderately cohesive. Theoretical and empirical runoff erosion models commonly assume capacity transport (e.g. Kirkby 1971, 1980a, Carson and Kirkby 1972 pp. 207–219, Smith and Bretherton 1972, Hirano 1975), but such assumptions often overestimate actual transport rates severalfold (Dunne and Aubrey 1986). Due to the cohesion and the small sand-sized component of badland regoliths, coupled with the steep slope gradients, runoff and interflow are likely to carry bed sediment loads well below capacity.

A few researchers have recognized that flow on steep slopes is commonly detachment limited and suggest that the detachment (or deposition) by the flow D_f is related to an intrinsic detachment capacity D_c (for zero sediment load), the actual sediment load G and the flow transport capacity T_c (Foster and Meyer 1972, Meyer 1986, Lane et al. 1988, Foster 1990)

$$D_f = D_c(1 - G/T_c) \tag{10.6}$$

This relationship implies an interaction between deposition and entrainment on the bed. However, rills and badland slopes seldom show evidence of sediment redeposition or partial surface mantling until flow reaches alluvial washes or alluvial surfaces (miniature pediments). The downstream transition from bare regolith to sand- and silt-mantled alluvial surfaces is generally abrupt (Schumm 1956a, b, Smith 1958, Howard 1970). The high roughness and possibly the greater grain rebound on badland regolith may make transport capacity greater than for an alluvial surface at the same gradient (Howard 1980). This suggests that on steep badland slopes and rills actual detachment D_f can reasonably be assumed to equal the intrinsic detachment D_c. This approach is used in the following models.

Howard and Kerby (1983) successfully related areal variations in observed rates of erosion of bedrock channels on shales to the pattern that would be expected

if erosion rates were determined by dominant shear stress in the channel. Following Howard (1970) they suggested that erosion rate $\partial y/\partial t$ (detachment rate) is determined by shear stress τ:

$$\frac{\partial y}{\partial t} = K_c(\tau - \tau_c)^\beta \tag{10.7}$$

where τ_c is a critical shear stress, β is an exponent, and the constant of proportionality K_c depends upon both flow durations and bedrock erodibility. Foster (1982) and Foster and Lane (1983) assume a similar relationship (with $\beta = 1$) for rill detachment capacity. Numerous experiments on fluvial erosion of cohesive deposits indicate scour rates that correlate with the applied shear stress (Parthenaides 1965, Parthenaides and Paaswell 1970, Akky and Shen 1973, Parchure and Mehta 1985, Ariathurai and Arulandan 1986, Kuijper et al. 1989, Knapen et al. 2007). Assuming certain hydraulic geometry and resistance equations, and further assuming that the dominant values of shear stress greatly exceed the critical value, then Equation (10.7) can be re-expressed as a function of local gradient S and contributing drainage area A_d (Howard 1994b, 1997, 2007):

$$\frac{\partial y}{\partial t} = K_c(K_e\ A_d^m\ S^n - \tau_c)^\beta \tag{10.8}$$

where the constant of proportionality, K_e, likewise depends upon constants in the hydraulic geometry equations. Theoretical values for m and n for the assumed hydraulic geometry relationships are $\sim$0.3 and $\sim$0.7, respectively, with observed values being 0.45 and 0.7.

In some badland washes and in much of the throughflow in badland regolith the limiting factor may be the rate of decrease of shear strength of surface rinds either due to weathering of the bedrock or to wetting and dispersion of regolith crusts and shards. Even though the weathering rate is a limiting factor, flow conditions can still affect erosion rates, as illustrated in a simple model by (Howard 1994a, 1998) that assumes that flocs can be removed when weathering, progressing from the surface inward, reduces cohesion to below the applied shear stress. The resulting erosion rate increases as a joint function of shear stress and intrinsic weathering rate.

Both of these models suggest an erosion rate that increases with some measure of the strength of the effective flow. However, data on erosion rates in badland channels is limited, and that on the accompanying flow is essentially nonexistent.

In some cases flow in bedrock rills may become so sediment laden that they exhibit Bingham flow properties with development of levees on rills and depositional mudflow fans. The common occurrence of localized slumps and draping flows on badland slopes might be appropriately characterized by Bingham flow as well.

Requisite conditions for rill development and the overall control of drainage density in badlands has been a continuing theme in badlands geomorphology, starting with Schumm's (1956a) introduction of the 'constant of channel maintenance', a characteristic length from the divide to the head of rills. Rills have been discussed in two contexts. The first is the critical hydraulic conditions required for the transition from dispersed overland flow to channelized rill flow (see general discussions in Bryan 1987, Gerits et al. 1987, Rauws and Govers 1988, and Torri et al. 1987). Several criteria have been proposed, including critical slope gradients (Savat and De Ploey 1982), a critical Froude number (Savat 1976, 1980, Savat and De Ploey 1982, Hodges 1982, Karcz and Kersey 1980), and a critical shear stress or shear velocity (Moss and Walker 1978, Moss et al. 1979, 1982, Savat 1982, Chisci et al. 1985, Govers 1985, Govers and Rauws 1986, Rauws 1987). On the steep badland slopes with strongly channelized flow in cracks, microrills and pipes much of the flow on badland slope exceeds critical conditions for rill initiation by any of these criteria. Rill initiation on badland slopes has also been related to unroofing of tunnels and micropipes (Hodges and Bryan 1982) which may be related as much to saturation, swelling and softening of badland regolith as to the hydraulic factors mentioned above (see Fig. 10.5, Gerits et al. 1987, Imeson and Verstraten 1988).

Runoff thus seems to be capable of rill initiation over most of badland slope surfaces, with the possible exception of well-cemented sandstone layers with thin regoliths. The development and maintenance of semipermanent rills requires a balance between the tendency of runoff to incise and other processes that tend to destroy small rills (Schumm 1956a, Kirkby 1980b). Such processes include shrink-swell of the surface layers, which destroys microrills (Engelen 1973), needle-ice growth (Howard and Kerby 1983), mass wasting by creep and shallow slides (Schumm 1956a, b, Howard

and Kerby 1983) and rainsplash (Howard 1970, Moseley 1973, Dunne and Aubrey 1986). On badlands in humid climates a well-defined seasonal cycle of rill creation and obliteration occurs (Schumm 1956a, Howard and Kerby 1983). In arid regions advance and retreat of rill systems on slopes may occur over much longer time scales, but may also be dramatically altered by a single heavy summer rainfall or a winter mass-wasting event. In the discussion below the emphasis is on 'permanent' rills and gullies that have persisted long enough to have created well-defined valleys. In the simulation modelling discussed below the location of permanent rills is determined by the balance between runoff erosion using Equation 10.8 and diffusive processes (rainsplash or mass-wasting).

Badland Architecture and Evolution

This section emphasizes the spatial process variations that determine the overall architecture of both slope and channel features of badlands. Furthermore, the temporal evolution of badlands will be examined both through reference to the specific case of the Henry Mountains area and through the use of simulation models.

Evolution and Areal Distribution of Badlands

The rapid erosion of badland slopes means that they occur only where high relief has been created in shaly rocks. In the Henry Mountains area this has occurred through erosional removal of a protective caprock or through rapid master stream downcutting. The ramparts of sandstone cuestas feature local badlands in sub-caprock shales, and more extensive badland areas occur where buttes have been recently denuded of their caprock. However, the badlands on cuesta ramparts are well developed only during relatively arid epochs (such as the present) when mass-wasting of caprocks is relatively quiescent (see discussion in Chapter 8).

The master stream is the Dirty Devil-Fremont River system which, during the Quaternary, has had a history of alternating stability or slight aggradation during pluvial epochs with rapid downcutting, followed by stability at the close of non-pluvial epochs (Howard 1970, 1997). During the pluvial epochs the stable base level coupled with physical weathering and mass-wasting of the sandstone cuestas resulted in development of extensive talus slopes on the ramparts of the escarpments coupled with gravel-veneered alluvial surfaces (pediments) mantling the shales. Thus badlands were rare during pluvial epochs, probably occurring only locally on scarp ramparts or caprock-stripped buttes. The post-pluvial (Bull Lake) dissection of river terraces and alluvial surfaces underlain by Mancos Shale has created the spectacular badland landscape near Caineville, Utah (Fig. 10.1). The river apparently downcut about 65 m shortly after the close of the Bull Lake pluvial (of Early Wisconsin age, Anderson et al. 1996), followed by stability at about its present level (Howard 1970, 1997). As a result, a wave of dissection has moved headwards towards the sandstone cuestas to which the alluvial surfaces were graded, producing a sequence of landforms from scattered Bull Lake alluvial surface remnants near the scarps (remaining primarily where the capping gravels were thickest) through a zone of high-relief (50 to 60-m) badlands to modern alluvial surfaces near the master drainage where the badlands have been completely eroded (Fig. 10.11). Shale areas that are either remote from the master drainage or have been protected from stream downcutting by downstream sandstone exposures are either undissected Pleistocene alluvial surfaces or very-low-relief badlands.

Similar post-glacial downcutting has been implicated in forming the shale badland landscapes of the Great Plains of the United States and Canada (Bryan et al. 1987, Campbell 1989, Wells and Gutierrez 1982, Slaymaker 1982), with a similar progression from undissected uplands (often capped by a protective grassland cover) through high-relief badlands to modern alluvial surfaces. In semi-arid and humid regions, badlands occur primarily where a former vegetation has been removed from shales or easily eroded regolith. Thus such occurrences are similar to relief generation through a protective caprock and its subsequent removal.

Relationship Between form and Processes

Badlands exhibit a surprisingly wide range of slope form. A contrast between steep, straight-sloped badlands with very narrow divides and a convex form with generally gentler slopes was noted quite early in the

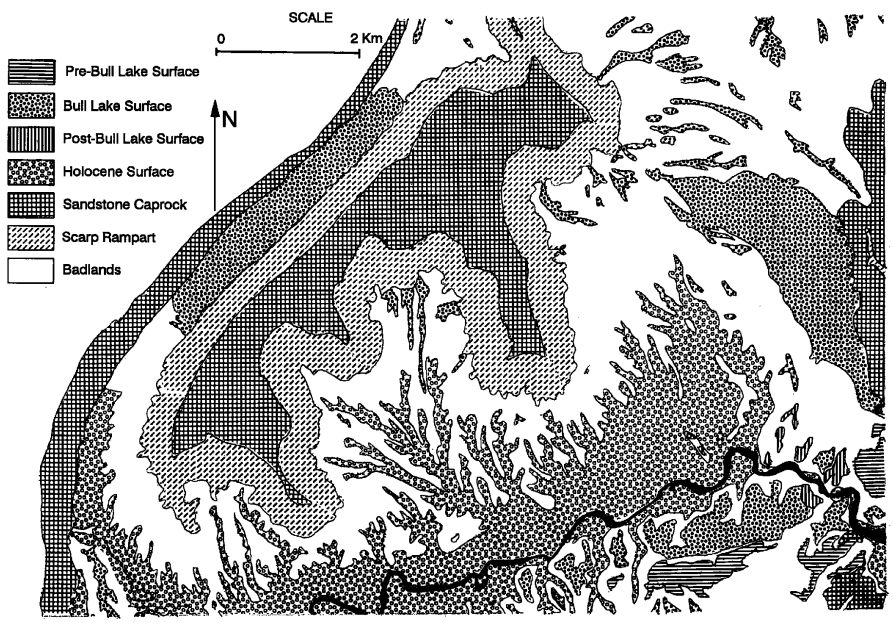

Fig. 10.11 Geomorphic map of part of the Caineville Area, near the Henry Mountains, Utah. Bull Lake surfaces are Early Wisconsin in age. Bull Lake surface includes terraces of the Fremont River and alluvial surfaces graded to these terraces. The Fremont River is the black sinuous line near the bottom of the illustration. The large area of Bull Lake surface at the right edge is preserved because it drains across a sandstone caprock that acts as a local baselevel. Pre- and Post-Bull Lake surfaces are Fremont River terraces. Holocene surface is Fremont River floodplain and alluvial surface graded to modern river level. Scarp rampart includes both rockfall-mantled shale and high-relief badlands (based on Howard 1970 Plate 6)

literature on badlands and is exemplified in the classic South Dakota badlands by slopes in the Brule and Chadron formations, respectively (Schumm 1956b). In the Henry Mountains area a similar contrast occurs between badlands on the Mancos Shale and those in the Morrison Formation (compare Figs. 10.1 and 10.2). Badlands in the Summerville Formation are similar to the Mancos Shale badlands in having straight slopes and narrow divides, but they have significantly lower maximum slope gradients (Table 10.1). Many badlands have quite complicated slope forms due to contrasting lithology and interbedded resistant layers (e.g., the Dinosaur badlands of Canada). Occasionally, pinnacle forms of badlands are found that are characterized by extremely high drainage density, knife-edge divides, and generally concave slope form (Fig. 10.12). The following discussion of badland erosional processes links these differences in slope form to variations in lithology and climate.

The broadly rounded upper slopes of the Morrison, Chinle, and Chadron formations are probably due to creep processes (see above). The popcorn texture of surface aggregates allows relatively large relative movements of the aggregates as their edges become wet and slippery. However, lower sideslopes sometimes exceed 40°, locally resulting in rapid flowage of the popcorn surface layer off the slope. This results in long, narrow tracks of exposed subsoil on the lower slopes which rapidly develop a new surface layer of popcorn aggregates. Convex slopes develop through creep in any circumstance where the creep rate increases monotonically with slope gradient and where

Table 10.1 Comparison of slope angles (in degrees) on badlands in Mancos Shale, the Summerville Formation, and the Morrison Formation

Formation	Angle-of-repose slopes[1]	Unstable slopes[2]	Average slope angle[3]
Summerville	31.5	31.7	27
Mancos	32	34.8	40
Morrison	–	34.8	–

[1]Slopes constructed of unweathered shale shards.
[2]Constructional talus slopes of mass-wasted regolith below vertical cliffs in shale.
[3]Average gradient of long natural slopes in areas of moderate to high relief.

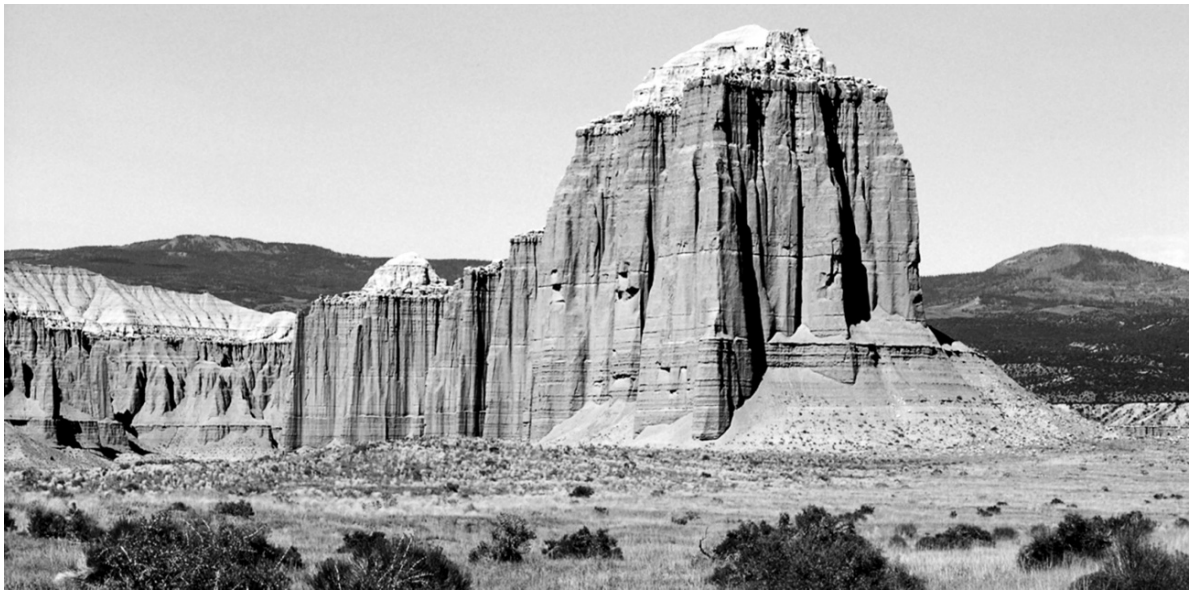

Fig. 10.12 Pinnacle badland slopes in Cathedral Valley, near Caineville, Utah. The steep slopes were formerly protected by a caprock. Note the low-gradient slopes in the same formation at the base of the slope (Entrada Sandstone) (photo by A. Howard)

creep is the dominant erosional process; this was first elaborated by Davis (1892) and Gilbert (1909).

Even on these rounded slopes runoff erosion becomes increasingly important downslope, becoming dominant in rills and locally within shallow pipes and cracks in the thin regolith.

The Mancos badlands have a nearly linear profile with narrow, rounded divides, which range in width from less than 0.5 m in high-relief badlands to 1–2 m in low-relief areas (Fig. 10.1). Because of the very thin regolith on these narrow divides and a tendency for development of a shale-chip surface armoring, Howard (1970) and Moseley (1973) attributed the divide rounding to rainsplash. This process is effective on narrow divides even at low gradient because the maximum splash distance is greater than the divide width.

Virtually all high-relief badland slopes in the Henry Mountains region have nearly constant gradient on their lower portions, even on the broadly convex slopes in the Morrison Formation. These maximum gradients are usually within a few degrees of the angle of repose of dry detritus weathered from the formations. Maximum gradients on the Summerville Formation, with its loose weathered layer, are 3–5° less than the angle of repose, probably due to seepage flow decreasing the maximum stable slope angle (implied in Equations (10.1, 10.2, 10.3, 10.4 and 10.5); see Lambe and Whitman 1969, p. 354). However, in the Morrison and Mancos badlands the slopes are 3–10° higher than the repose angle for loose weathered shale due to cohesion. Consequently, many lower slopes are on the verge of failing by flowage and slipping. Many such slopes do occasionally fail, involving only the thin surface layer (5–10 cm) and leaving long, narrow tracks of exposed subsoil on the lower slopes. Such flows are numerous on steep slopes on the Morrison and Summerville Formations, but are rare on the Mancos badlands. However, on the Mancos badlands, whole sections of hillside appear to slip or slump short distances downhill during rainstorms, producing tension cracks arranged in waves suggesting differential movement and, rarely, extensive shallow slumping (Fig. 10.13). Tension cracks are the more numerous and wider the steeper the gradient, particularly on slopes undercut by meandering washes.

On low-gradient portions of slopes, creep-like movement of the surface layer predominates, which is generally modeled as a linear function of slope gradient (Culling 1963, Carson and Kirkby 1972, Howard 1994b, Fernandes and Dietrich 1997). However, for the gradients approaching the limiting slope angle (which in actuality is temporally and spatially

Fig. 10.13 Steep Mancos Shale slopes showing evidence of accelerated rate of mass wasting. The regolith mass at "@" derived from the scar immediately above. Elsewhere in this picture are numerous scars and regolith masses suggestive of episodic slumping or flow. New regolith rapidly forms whenever it becomes exposed. Contrast the lack of rills on this slope with the Mancos Shale slopes in Fig. 10.1 (photo by A. Howard)

variable), mass wasting rates can be functionally represented by a rapid rate increase (Kirkby (1984, 1985b), Howard (1994b), Roering et al. 1999, 2001a, b).

Nearly linear lower slopes on regolith-mantled, high-relief badlands would be expected if mass-wasting determines slope form. Close to the divide, where creep rates are low (due to modest amounts of regolith supplied from upslope) and corresponding gradients are low, mass wasting rate follows the sine relationship. Consequently, gradients increase rapidly downslope. Rainsplash erosion is also a diffusive process, producing divide convexity. As the total volume of mass wasting debris increases downslope, equivalent rates of erosion may require gradients approaching the limiting slope angle where slippage or flowage becomes important. In these lower slope regions the incremental addition of weathered material along the slope can be accommodated by a very slight increase in gradient, thereby creating a nearly straight profile. Such lower slopes are essentially equivalent to the threshold slopes of Carson (1971) and Carson and Petley, (1970) except that they are probably best modelled by a rapid but continuous increase in mass wasting rate as the limiting angle is approached rather than by an abrupt threshold (Howard, 1994b, Roering et al. 2001a).

Indirect evidence for threshold slopes in steep badlands comes from areal variations in badland form. Average hillslope gradients in badlands of the Summerville and Mancos Formations show little variation with slope length except for very short slopes (Fig. 10.14). However, the drainage density exhibits a complicated relationship to relief ratio, generally increasing with relief ratio up to a value of about 0.5, but decreasing in very high relief badlands (Fig. 10.15). The relatively low drainage density of areas with very high relief ratio may be explained by the onset of sliding and slumping on steep slopes. In areas of high relief large increases of the rate of erosion of a slope at its base should be accompanied by only a slight change in slope gradient (Fig. 10.14). But the small increase

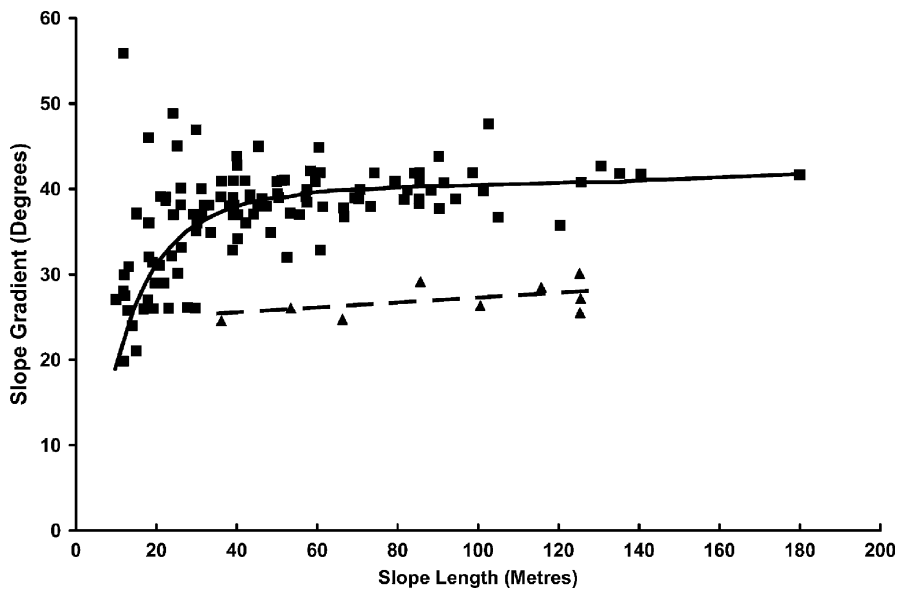

Fig. 10.14 Plot of hillslope gradient versus slope length in badlands in the Summerville (*triangles*) Formation and Mancos Shale (*squares*) (based on Howard 1970, Fig. 43). The short slopes with very high gradients occur on undercut banks along meandering washes

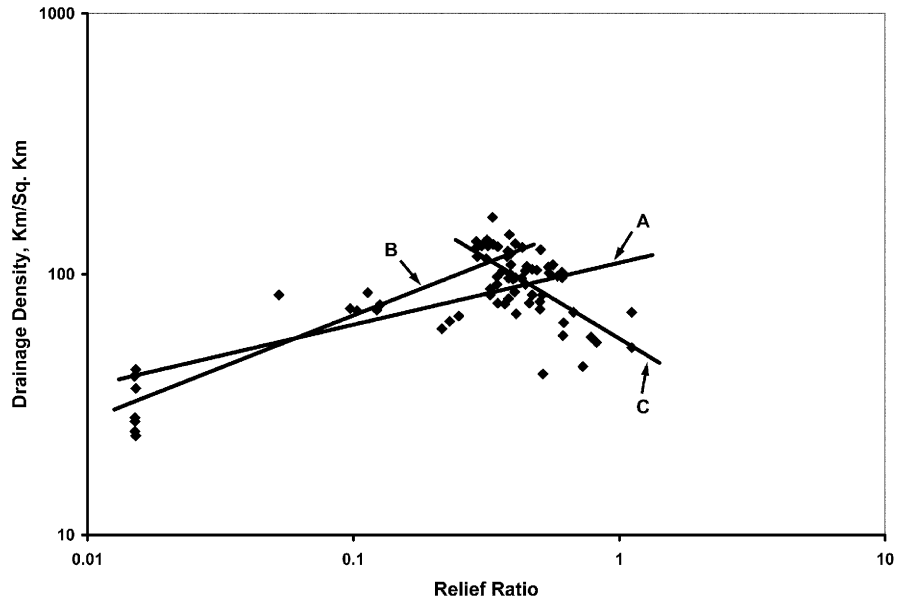

Fig. 10.15 Drainage density versus relief ratio for badland areas on Mancos Shale. Measurements made on areal photographs with a scale of approximately 1:12,000. Relief ratio determined by inscribing a 150 m diameter circle around a badland divide and measuring the maximum relief photogrammetrically and dividing by 75 m. Drainage density is defined as total length of all hollows and valleys visible on the photograph in the circle divided by the area of the circle. Ephemeral rills lacking defining ridge lines are not included. Regression lines are A for all points, B for values of relief ratio less than 0.35 and C for values greater for 0.2. All are statistically significant

in slope angle increases the efficiency of erosion on the slope relative to the channel, so that the critical drainage area necessary to support a channel increases, with a resulting decrease in drainage density. Average slope length L and drainage density D are related to the average slope angle θ by (Schumm 1956a, p. 99)

$$L \operatorname{Cos} \theta = 2/D. \tag{10.9}$$

Because slope angles vary little with relief ratio in steep badlands, the decrease in drainage density accompanying increase in relief ratio is accompanied by a proportional increase in slope length. This decrease in drainage density with increasing erosion rates for landscapes with threshold slopes has been theoretically justified and demonstrated in simulation modeling by Howard (1997) and Tucker and Bras, (1998). By contrast, in areas of low overall gradient, increase in relief ratio is accompanied by increases in drainage density. Therefore, slope length decreases nearly in proportion since the cosine term is near unity. Modelling by Howard, (1997) suggests that this occurs when slopes are eroded by classic linear diffusion and channel erosion occurs with shear stresses not much above the threshold of detachment (τ_c in Equations 10.7 and 10.8).

At least four types of surfaces occur on badlands: (1) slopes with exposed bedrock; (2) regolith-mantled slopes; (3) Rills and washes with exposed bedrock; and (4) alluvium-mantled surfaces. These surfaces generally sharply abut against each other, with the transitions corresponding to thresholds in the relative importance of processes. Most badland slopes are regolith-mantled, albeit shallowly. However, on steep slopes or where bedrock is resistant to weathering the surface is irregular, expressing variations in weathering characteristics of the rock, jointing, and stratigraphy (Fig. 10.16). In contrast, minor differences in lithology of the rocks underlying regolith-mantled badlands (non-undercut areas in Fig. 10.13) do not affect slope form, for the geometry is determined by processes of downslope transport of the weathered debris. The threshold between bare and regolith-mantled slopes is commonly equated with weathering- versus transport-limited conditions, respectively (Culling 1963, Carson and Kirkby 1972 pp. 104–106). However, there are

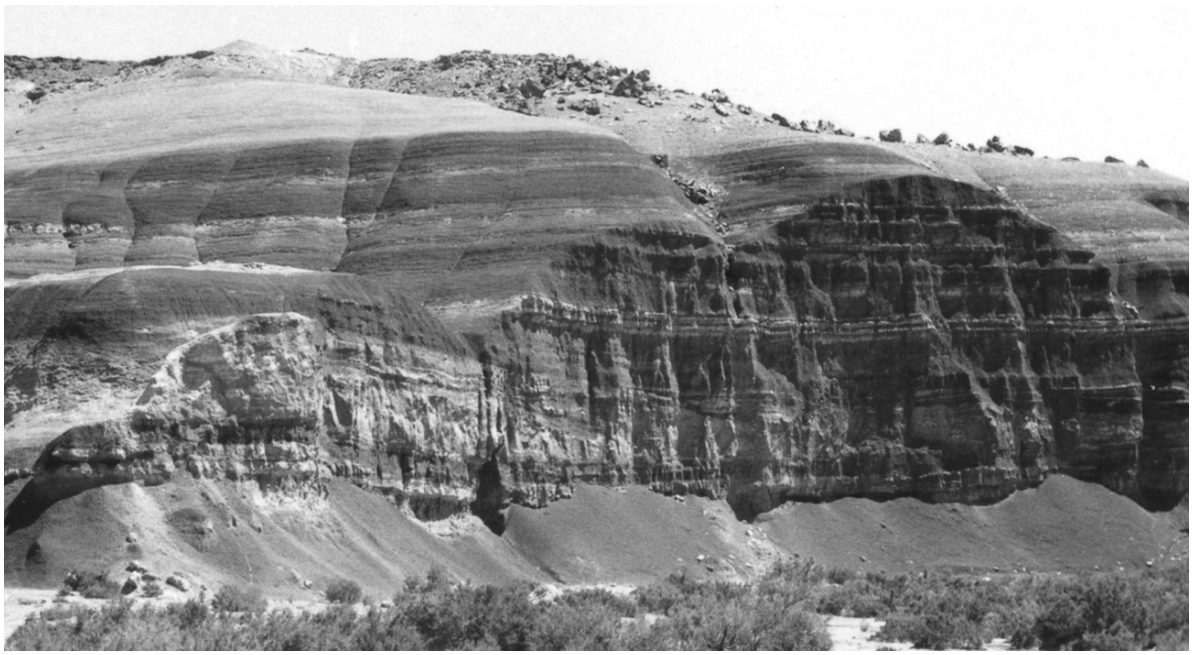

Fig. 10.16 Near-vertical slopes in shale of the Morrison Formation formed by past undercutting by the Fremont River. Differences in bedding are strongly expressed in vertical slopes in contrast to the smoother, gentler slopes mantled by 20+ cm of regolith (photo by A. Howard)

four factors that may limit overall slope erosion rate, the potential weathering rate PW, the potential mass wasting rate PM, the potential detachment rate by runoff (combined splash and runoff detachment) PD, and the potential fluvial transport rate PT. On regolith-mantled slopes $PW > (PM + PD)$ and $PD < PT$. Either mass-wasting or runoff detachment may be quantitatively dominant on such slopes; measurements by Schumm (1963) suggest runoff dominance. The use of the term transport-limiting for these mantled slopes is inaccurate, because the runoff component of erosion is detachment- rather than transport-limited. Bare bedrock slopes have $PW < (PM + PD)$ and $PD < PT$, so that the term weathering-limiting is appropriate. Alluvial surfaces have $PD > PT$, and generally $PM \approx 0$ because of the low gradients. Bedrock-floored rills and washes have similar conditions to bare rock slopes except that $PM \approx 0$. The rock-mantled slopes considered in Chapter 9 would appear to be similar to badland regolith-mantled slopes. However, the surface layer is often a lag pavement that greatly restricts runoff erosion, so that the overall rate of erosion is often determined either by (1) the rate of breakdown of the pavement by weathering or (2) the rate of upward migration of fines due to freeze-thaw or bioturbation, or (3) mass-wasting rates.

The supply of moisture is the primary factor determining the weathering rate of the soft rocks forming badlands. For vertically falling precipitation the interception per unit surface area of slope diminishes with the cosine of the slope angle (in actuality some water attacks vertical or overhanging slopes, for escarpment caprocks often project beyond underlying shales). This suggests that a critical gradient separates mantled slopes on which rates of mass wasting increase with slope gradient from steeper bedrock slopes which erode less rapidly as gradients increase (at least until slope relief is great enough to cause bulk failure in the shale bedrock).

Badlands with steep slopes and exposed bedrock commonly develop pinnacle forms (alternatively termed needle-like, serrate, or fluted) (Fig. 10.12). Examples include the Brice Canyon pinnacles, the badlands described by Carman (1958), the spires of Cathedral Valley, Utah, and portions of the badlands of South Dakota. Pinnacle badlands commonly are

initiated as a result of near-vertical slopes developing in non-resistant shales lying beneath a resistant caprock which erodes very slowly as compared to downwearing in the surrounding badlands. Eventually the caprock is weathered away or fails, and the underlying shales rapidly erode, developing the fluted form due to rapid rill incision because of the steep relief. Drainage densities are exceedingly high on these slopes and owing to the absence of a mantling regolith and mass wasting processes divides are knife-edged. Slope profiles are generally concave, indicating the dominant role of runoff (both unconcentrated and in rills) in erosion. Although the steepness of the fluted slopes is partially due to the high initial relief, the slopes at divides generally steepen during development of fluted badlands because rill erosion rapidly erodes slope bases and weathering and erosion rates on sideslopes decrease with increasing slope gradient due to less interception of moisture. As the fluted slopes downwaste, they are generally replaced by mantled badland slopes with lower drainage density at a very sharp transition, as a Bryce Canyon.

Fig. 10.17 Runoff on alluvial surfaces on Morrison Formation Shales. Photo was taken during waning flow stages (photo by A. Howard)

Fluvial Processes and Landforms of Badland Landscapes

Howard (1980) distinguished three types of fluvial channels, bedrock, fine-bed alluvial, and coarse-bed alluvial. In most cases these types of channel are separated by clear thresholds in form and process. In badlands coarse-bed alluvial channels usually occur only where gravel interbeds are present.

Alluvial Surfaces

Few contrasts in landscape are as distinct as that between badland and alluvial surfaces on shaly rocks. Low-relief, alluvium-mantled surfaces in badland areas have been referred to by a variety of names, including miniature pediment (Bradley 1940, Schumm 1956b, 1962, Smith 1958), pseudo- and peri-pediment (Hodges 1982), and alluvial surface (Howard 1970, Howard and Kerby 1983). The last term is used here because of its neutral connotation regarding the numerous and conflicting definitions of ‘pediment’.

Flow on alluvial surfaces is either unconfined or concentrated in wide, braided washes inset very slightly below the general level of the alluvial surface (Fig. 10.17). Alluvial surfaces may be of any width compared to that of the surrounding badlands, contrasting with the confinement of flow in bedrock rills and washes. The alluvium underlying most alluvial surfaces is bedload carried during runoff events and redeposited as the flow wanes, but adjacent to major washes overbank flood deposits may predominate. Although the surface of alluvial surfaces and washes is very smooth when dry, during runoff events flow is characterized by ephemeral roll waves and shallow chute rilling which heals during recessional flows (Hodges 1982).

An alluvial surface and badlands commonly meet at a sharp, angular discordance (Figs. 10.18 and 10.19). At such junctures slopes, rills and small washes with inclinations up to 45° abut alluvial surfaces with gradients of a few degrees. In most instances the alluvial surfaces receive their drainage from badlands upstream and are lower in gradient than the slopes or washes. The layer of active alluvium beneath an alluvial surface may be as thin as 2 mm, but increases to 10 cm or

Fig. 10.18 Sharp junction between steep badland slopes and alluvial surface in Mancos Shale. Arrows are at the level of Bull Lake terrace. Fremont River flows just in front of the terrace shown by the arrows (photo by A. Howard)

more below larger braided washes. Below the active alluvium there occurs either a thin weathered layer grading to bedrock or, in cases where the alluvial surface has been aggrading, more alluvium.

Generally alluvial surfaces and their alluvial washes obey the same pattern of smaller gradients for larger contributing areas. Howard (1970, 1980) and Howard and Kerby (1983) showed that the gradient of alluvial surfaces is systematically related to the contributing drainage area per unit width (or equivalent length) L in badlands both in arid and humid climates:

$$S = CL^z, \tag{10.10}$$

where the exponent z may range from -0.25 to -0.3. The equivalent length for washes on alluvial surfaces is simply the drainage area divided by the channel width, but on unconfined flow on smaller alluvial surfaces it is the drainage area contributing to an arbitrary unit width perpendicular to the gradient. The proportionality constant C can be functionally related to areal variations in sediment yield, runoff, and alluvium grain size. Howard (1980) and Howard and Kerby (1983) showed that the value of the exponent z is consistent with the assumption that alluvial surface gradients are adjusted to transport sand-sized bedload at high transport rates.

Badland alluvial surfaces are therefore comparable to sand-bedded alluvial river systems in general in that gradients decrease with increasing contributing area (downstream). The major contrast is the presence of unchannelled areas in the headward portion of alluvial surfaces. Their presence is probably related to the absence of vegetation and flashy flow, which discourages formation of banks and floodplains. The alluvial surfaces contrast with alluvial fans in that the former are through-flowing systems with only minor losses of water downstream and contributions of water and sediment from the entire drainage area. Furthermore, the alluvial surfaces are generally slowly lowering. If they are aggrading, they do so at a very slow rate. Thus the downstream spreading of discharge characteristic of alluvial fans (and deltas) generally does not occur on alluvial surfaces.

Alluvial surfaces are surfaces of transportation, with a gradient determined by the long-term balance between supplied load and discharge (Smith 1958). Thus they are graded surfaces in the sense of Mackin (1948). Howard (1982) and Howard and Kerby (1983) discussed the applicability of this concept in the context of seasonal and long-term changes in the balance of sediment load and discharge, and the limits to the concept of grade. Interestingly, most badland alluvial

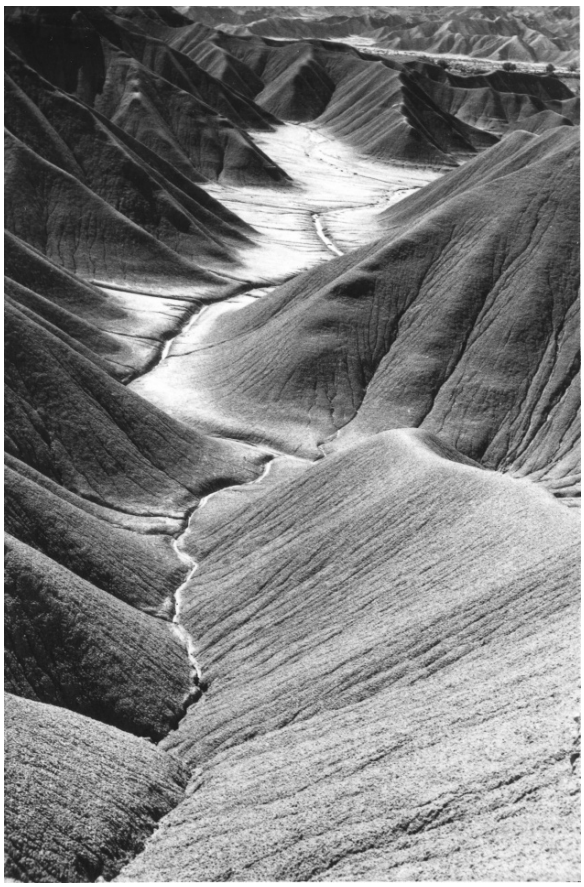

Fig. 10.19 Downstream transition between bedrock wash and alluvial surface in Mancos Shale badlands. Slope gradients are about the same whether grading to bedrock wash or to alluvial surface (photo by A. Howard)

surfaces slowly lower through time, as indicated both by direct measurements (Schumm 1962, Howard and Kerby 1983) and by the presence of rocks on pedestals of shale surrounded by an alluvial surface that has lowered around it. Thus the alluvial surfaces are not destroyed by slow lowering of base level, but they become readily dissected by bedrock washes if base level drops too rapidly (Fig. 10.20). Howard (1970) and Howard and Kerby (1983) present evidence that larger alluvial channels are capable of more rapid erosion than smaller ones without being converted to bedrock channels. Howard and Kerby (1983) suggest that the maximum erosion rate is proportional to about the 0.2 power of drainage area. It is uncertain whether the erosion (or aggradation) rate on alluvial surfaces systematically influences their gradients.

Bedrock Channels

Badland washes and rills are usually floored by slightly weathered bedrock. Beneath the smallest rills the weathered zone is about as thick as that on adjacent unrilled slopes, although this thickness varies with the seasonal rill cycle (Schumm 1956a, 1964, Schumm and Lusby 1963). In larger badland washes, weathering products are rapidly removed, exposing bedrock. Deposits of alluvium occur only locally in scour depressions. Larger bedrock washes often display marked meandering with the wavelength increasing systematically with the 0.4 power of drainage area (Howard 1970), which is consistent with meander wavelength in alluvial streams. In contrast to the alluvial surfaces, the gradient of bedrock washes is not uniquely related to the size of contributing drainage area and their gradient is steeper than alluvial washes of equivalent area (Howard 1970, Howard and Kerby 1983).

Slope-Channel Interactions in Badlands

Erosion in large bedrock streams may be nearly independent of the sediment load supplied by slope erosion (e.g., Equations 10.7 and 10.8), so that the nature of the surrounding slopes has minor influence on stream erosion rates. Thus, in general, evolution of hillslopes follows rather than leads that of the stream network. However, the low-order tributaries, including rills, interact with adjacent slopes and their gradients are largely determined by hillslope gradients. The smallest rills are ephemeral (Schumm 1956a, Schumm and Lusby 1963, Howard and Kerby 1983) and have gradients essentially equal to hillslope gradients.

The nature of hillslope-channel interactions is poorly understood. Permanent channels occur only where runoff is sufficient such that streams erode as rapidly as the surrounding slopes and with a lesser gradient. Diffusive processes (creep and rainsplash) are more efficient than channel erosion for small contributing areas. This is suggested by models of bedrock channel erosion (e.g., Equation 10.8) where, for a given erosion rate, gradients would have to approach infinity as contributing area approaches zero. In contrast, mass wasting slope processes and rainsplash function even at divides. Ephemeral rills are generally not inset into the slope because seasonal (or

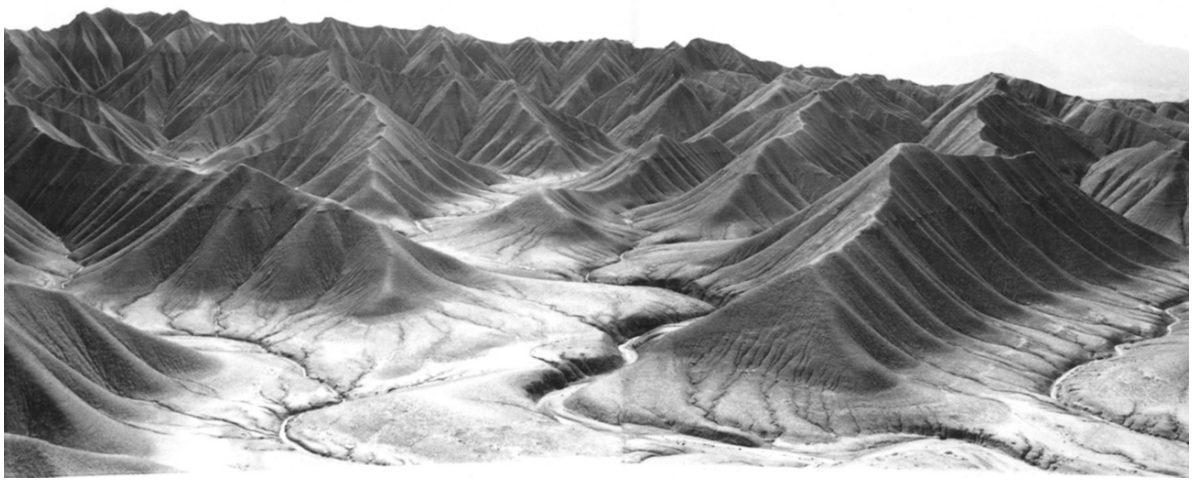

Fig. 10.20 Badlands and dissected alluvial surface in Mancos Shale. The former boundary between badland slopes and the alluvial surface occurred at the light-dark transition (photo by A. Howard)

year-to-year) mass wasting by needle ice or shallow slips and direct frost heaving episodically destroys them. Permanent rills and washes are distinguished by (and can be defined by) being inset within a definable drainage basin, so that they have a lower gradient than surrounding slopes. Even so, such permanent rills may occasionally be partially infilled by mass-wasting debris.

The sharpness of the junction between badland slopes and adjacent alluvial surface (e.g., Figs. 10.1 and 10.18) as well as its spatio-temporal persistence has fascinated generations of geomorphologists, and a variety of hypotheses have been offered for its origin and maintenance. Badlands rising from alluvial surfaces have gradients nearly equal to nearby slopes terminating at bedrock channels (Fig. 10.19), implying nearly equal rates of erosion, even though the alluvial surfaces may be stable or very slowly degrading. Moreover the slope form (straight-sided or broadly convex) remains the same. In Fig. 10.19 successive profiles across the valley in a downstream direction may be similar to changes in profiles through time at one location, assuming that the alluvial surface remains at a stable level. The alluvial surfaces expand at the expense of the adjacent slope, as measured by Schumm (1962).

Schumm (1962), Smith (1958), Emmett (1970), and Hodges (1982) suggested that the abrupt contact is created and maintained by erosion concentrated at the foot of the slope, due perhaps to spreading of discharge from the rills at the base of the slope (a type of lateral planation), re-emergence of interflow, and changes of flow regime (subcritical to supercritical) at the slope-alluvial surface junction. Engelen (1973) suggested that spreading of water emerging onto alluvial surfaces from ephemeral micro-rills may be as important as spreading flow from more permanent rills. Hodges (1982) provided experimental information and observations on flow on badland slopes, rills, and alluvial surfaces. These data indicate the complicated nature of flow on these surfaces, including ephemeral rilling of the alluvial surface.

Howard (1970) suggested that the abrupt change of gradient at the head of an alluvial surface can be maintained without recourse to special processes acting at this location. Simulation modelling of coupled bedrock and alluvial channel evolution (using an equation similar to Equation (10.8) for bedrock erosion) indicated that bedrock channels maintained a nearly uniform gradient as they downcut until they were abruptly replaced by alluvial surface when elevations dropped to the level that the gradients were just sufficient to transport supplied alluvium (Fig. 10.21, discussed below). Although these simulations were targeted to the bedrock channel system on badlands, a similar situation may pertain to unrilled badland slopes. Water erosion is the dominant erosional process at the base of badland slopes (Schumm and Lusby 1963) and may be governed by similar rate laws as permanent rills and washes. As noted above, most seemingly unrilled

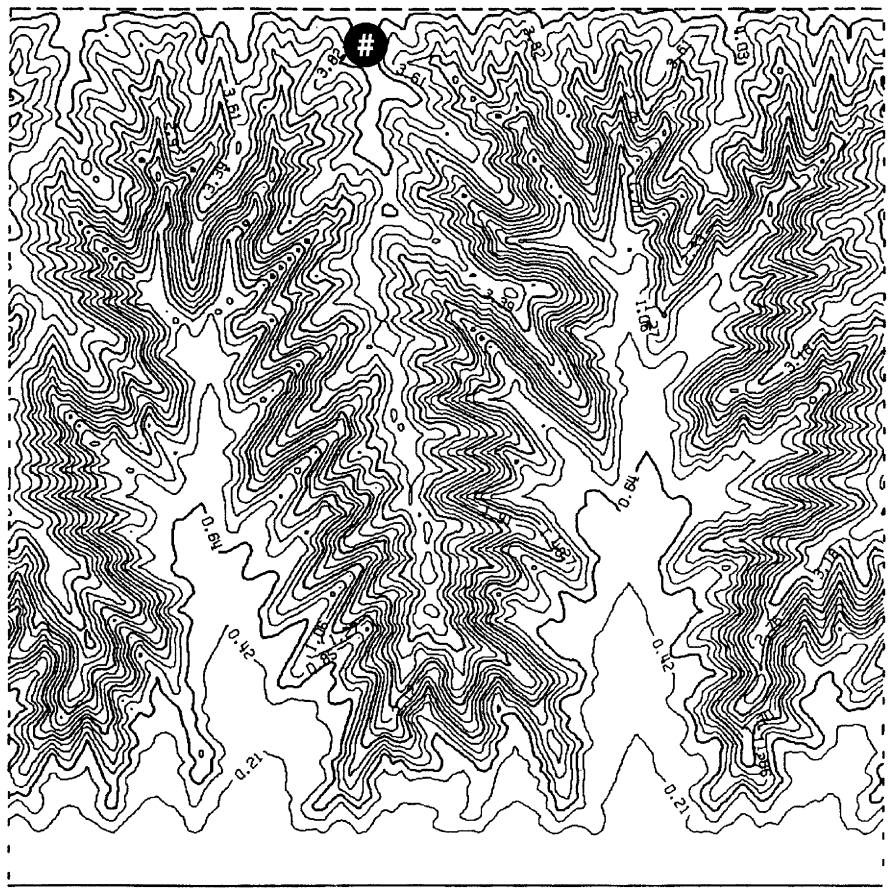

Fig. 10.21 Simulated badland landscape replicating the evolution of the Mancos Shale badlands near Caineville, Utah, based upon Howard (1997). Top boundary is a drainage divide, lateral boundaries are periodic, and bottom boundary is the base level control, conceived to be the Fremont River. The simulation started with initial conditions of a sloping alluvial surface at the level of the Bull Lake surface. Rapid incision then occurred to the modern level of the Fremont River followed by base level stability. The narrow divides near "#" are close to the level of the initial alluvial surface. Note that a new alluvial surface is extending headward from the fixed baselevel as badland slopes erode and retreat. As in Figs. 10.17 and 10.18, steep slopes are maintained as the badland slopes undergo nearly parallel retreat

badland slopes are primarily drained by concentrated flow either through an ephemeral surface network of crack flows (which are obliterated during the swelling and reshrinking of the surface layer) or as interflow in deeper cracks and micropipes.

Theoretical Models of Badland Evolution

There has been a rich history of quantitative modelling of slope and channel processes. These models have not primarily been directed towards specific issues related to badland slopes, but they have a general formulation that could be adapted to specific processes and materials in badlands. Early models were primarily applied to evolution of slopes in profile only, either for ease of analytical solutions or for numerical solutions with modest computational demands. A variety of approaches has been used, but two end members can be identified. Some investigators, as exemplified by the approaches of Kirkby (Kirkby 1971, 1976a,b, 1985a,b, Carson and Kirkby 1972, Kirkby and Bull 2000b) have attempted to quantify almost all of the processes thought to be acting on slopes and their distribution both on the surface and throughout the regolith. This approach offers the promise of detailed understanding of the spatio-temporal evolution of regolith and soils as well as the potential for addressing site-specific issues of erosion processes, slope hydrology, surface water geochemistry, and soil and water pollution. Some attempts have been made to apply such models to cover areal as well as profile characteristics of slopes, including issues of initiation of drainage (Kirkby 1986, 1990). However, the generality of such models restricts their use over large spatial or temporal domains due to present limitations of computer resources and the large number of parameters that must be specified.

Another approach has been to deliberately simplify models in order to address issues of drainage basin morphology and landscape evolution. Ahnert (1976, 1977) has been a pioneer in developing 3-D models of landscape evolution, although most of his efforts have

been directed to cross-sectional evolution of slope profiles (Ahnert 1987a,b, 1988). Recent advances in computer capabilities have permitted spatially explicit modeling of drainage basin evolution, and general reviews of these models are presented in Coulthard (2001) and Willgoose (2005). Typically these models include components for representing weathering, diffusive slope evolution by rainsplash and mass wasting, fluvial detachment, and sediment transport and deposition. Landform evolution models have been utilized, for example, to explore controls on drainage density (Howard 1997, Tucker and Bras 1998), effects of different processes of slope and channel coupling (Tucker and Bras 1998), effects of climate change and tectonic forcing (Tucker and Slingerland 1997, Coulthard et al. 2000, Tucker 2004, Gasparini et al. 2007), continental shelf incision during sea level lowstands (Fagherazzi et al. 2004), formation of alluvial fans (Coulthard et al. 2002, Garcia-Castellanos 2002), and incision of gullies (Howard 1999, Kirkby and Bull 2000a, Istanbulluoglu et al. 2005).

Howard (1997) applied a spatially explicit model to explore the evolution of the badland landscape in Mancos Shale discussed above. The model (Howard 1994b, 1997, 2007) incorporates bedrock weathering, diffusive mass wasting including enhanced transport rates as a critical slope steepness is approached (Roering et al. 1999, 2001a,b), shear stress dependent fluvial detachment (Equations 10.7 and 10.8), and sediment transport and deposition in alluvial channels using a bedload transport model. For the badland evolution simulations, weathering was assumed to be able to keep pace with erosion so that a regolith cover is assumed to be present on all slopes and regolith thickness is assumed not to be a limiting factor in determining the erosion rate. In accord with the observation that high relief Mancos Shale slopes are nearly linear in profile and exhibit instability suggestive of rapid mass wasting near the limiting angle of regolith stability (e.g. Fig. 10.13), the badland slopes were modelled such that they were eroding in the region of strong non-linear dependence of erosion rate on gradient. See Howard (1994b, 1997) for model details.

The specific issue examined by Howard (1997) is which history of river incision by the Fremont River best explains the pattern of slopes and alluvial surfaces in the Mancos Shale badlands in the area shown in Fig. 10.11. The existence of broad modern alluvial surfaces grading to the Fremont River coexisting with high-relief badlands created by dissection of an Early Wisconsin alluvial surface was postulated by Howard (1970) to be best explained by fairly rapid downcutting from the Early Wisconsin level of the Fremont river about 60 m above the present level to the level of the modern river followed by subsequent relative stability of base level. This scenario was explored in simulation modelling and compared with an alternative hypothesis that the river level lowered gradually from its Early Wisconsin level. Figure 10.21 shows the result of a simulation with the preferred hypothesis of rapid downcutting followed by stability. In early stages during the rapid downcutting, incision occurs first near the base level control (the lower boundary, corresponding to the Fremont River), with high relief slopes and steep channels gradually extending further inland. Extensive areas of nearly undissected original alluvial surface remained in headwater areas. Following cessation of downcutting, the downstream channel gradients decline until they reach a transport-limited condition. At this point an alluvial surface develops and extends headward, gradually replacing the badland slopes which undergo nearly parallel retreat (Fig. 10.20). The simulation duplicates the expected pattern of remote divides remaining near the level of the Early Wisconsin alluvial surface (e.g., at "#" in Fig. 10.20), high relief badlands occupying most of the simulation domain away from the main drainage (the lower boundary of the simulation domain), and an advancing modern alluvial surface near the main drainage. Simulations with gradual lowering of the river level failed to produce broad modern alluvial surfaces coexisting with high-relief badlands.

Landform evolution modeling of badlands thus has the potential to investigate both the landscape morphology resulting from different sets of process assumptions as well as different evolutionary scenarios.

Gullies

Localized accelerated erosion, including gully erosion, is a recurrent problem in most landscapes with deep regolith or soft bedrock. Gullying is most commonly associated with landscapes with climates near the semi-arid to arid transition or in regions with strongly

seasonal precipitation where rapid erosion is triggered by disruption of the vegetation cover by agricultural mismanagement, construction activities, fire, local landslides, or climatic change. However, rilling and gullying can occur even in humid climates with an erodible substrate lacking a coherent vegetation cover. Badlands can be viewed as the extreme end of gullying in which large areas become intensely dissected with sparse vegetation.

At the small end of the size spectrum agricultural fields are commonly plagued by rilling and ephemeral gullies (gullies small enough to be filled in by yearly ploughing, e.g., Poesen et al. (2006)). At the large end of the spectrum are incised river channels (e.g. Schumm et al. 1984, Wang et al. 1997, Darby and Simon 1999). The emphasis here will be in the middle scale, where localized deep incision attacks valley slopes and low-order valleys. General reviews of gullying are provided by Bull and Kirkby (1997), Poesen et al. (2003, 2006), and Valentin et al. (2005), including issues of mitigation and societal impacts not emphasized by this review that emphasizes gullying processes and the role of gullies in landform evolution.

Role of Vegetation

The discussion here will concentrate on the most common circumstance where channelized incision occurs through a vegetated substrate into weak subsurface regolith or sediment. Gully erosion generally initiates when applied fluvial shear stresses exceed the strength of the vegetation cover, and the vegetation is unable to recover between flow events. Thus erosion can occur when the shear resistance of the vegetation is diminished or as a result of increased stress from overland flow due to change in infiltration capacity or topographic changes concentrating flow, and less commonly, to extreme storm events. Once accelerated erosion has been initiated, return to a normal rate of erosion on all parts of the landscape may not occur until specific restorative actions are taken, such as seeding, fertilization, surface stabilization, grade control structures, and land recontouring. Incised valley bottoms are eventually stabilized due to lowered erosion rates and enhanced moisture availability (e.g., Ireland et al. 1939). In some landscapes natural revegetation on gully walls and headcuts occurs when slope gradients drop below critical values for rapid failure or when a year or two of frequent, low intensity rainstorms encourages vegetation establishment (e.g., Harvey 1992, Alexander et al. 1994). Gully systems considered here develop in low-order channels, headwater hollows, and the lower portions of slopes (e.g., Fig. 10.22).

In most landscapes in humid climates the natural vegetation significantly restricts erosion by runoff due to root cohesion, an open soil structure that encourages infiltration, and a high surface roughness that diminishes runoff velocity (Thornes 1985). The importance of this vegetative cover is made apparent when it is removed during construction, when erosion rates may increase by a factor of several hundred to ten thousand (Guy 1965, 1972, Wolman 1967, Vice et al. 1968, Howard and Kerby 1983). The deep regolith present throughout much of the southeastern United States could only have developed beneath a protective vegetation cover persisting during much of the Cenozoic (Pavich 1989). Accelerated erosion in this region due to poor agricultural practices from colonial times through the beginning of this century transferred immense quantities of sediment from hillslopes to valley bottoms, often resulting in deep gullying and valley sedimentation of a metre or more (Ireland et al. 1939, Happ et al. 1940, Trimble 1974, Jacobson and Coleman 1986).

Vegetation cover is often undervalued in terms of its control over landscape evolution. Its resistance to erosion, however, may be of the same order of magnitude as the underlying bedrock. In the Piedmont region of

Fig. 10.22 A gully system advancing through a broad hollow in the coast ranges of Northern California east of Point Reyes, USA. Some revegetation of the channel bottom is occurring even though the gully headwalls are still advancing (photo by A. Howard)

the southeastern United States, bedrock is commonly exposed in low-order stream channels, whereas deep regolith occurs beneath slopes and divides. If these landscapes approximate steady state denudation, then erosion of the hillslopes beneath a vegetative cover by creep and water erosion occurs only as rapidly as bedrock scour in nearby channels.

A vegetated landscape can thus be viewed as a three-layer structure: a thin vegetation cover, a more erodible regolith, and underlying bedrock. In some cases either the outer or inner layer effectively may be absent as with unvegetated badlands in the case of the former or deep unconsolidated sediments in the case of the latter. Where bedrock is exposed both outer layers are absent. Such a three-layer structure is incorporated in the present model. In some cases it may be necessary to incorporate a more complicated structure. For example, the B-horizon in soils in the southeastern U.S. often has greater erosional resistance than the overlying A-horizon, producing appreciable scarps in the clay-rich layer during gully incision (Ireland et al. 1939). Hardpans, fragipan, calcrete, silcrete, and ferricrete layers may play similar roles in other soils (Poesen and Govers 1990).

Reduction of erosional resistance through disturbance of the vegetation cover, either directly by fire, cultivation, overgrazing, etc., or indirectly by landslides, is a common cause of accelerated erosion (Thornes 1985, Foster 1990). In some cases, the enhanced erosion may instead arise from high stresses imposed by storm runoff, in part due to higher specific runoff yield and reduced hydraulic resistance where vegetation density is diminished (Graf 1979, Bull 1997). In order for erosion to continue to the point of producing a gullied landscape, reestablishment of vegetation must be inhibited; this inhibition is the second requirement for a accelerated erosional regime. Several factors related to the rapid erosion following vegetation disturbance are responsible for this inhibition: physical undermining of vegetation by erosion; removal of the seed and nutrient reservoir of the upper soil layers, rapid drying of unvegetated soil, and high temperatures on sunlit soils, among others. The inhibition of vegetation recovery in areas of high erosion rates is incorporated in some ecological models (Williams et al. 1984, Biot 1990, Collins et al. 2004, Istanbulluoglu and Bras 2005).

Accelerated erosion may also be triggered by rapid entrenchment of master drainage channels, creating migrating knickpoints on tributaries that encroach into headwater hollows and slopes. The entrenchment may be due either to human interference, such as channelization (e.g., Daniels 1960, Daniels and Jordan 1966) or overgrazing, or to climatic change (e.g., Brice 1966, Faulkner et al. 2007); a general review of the controversy surrounding climatic versus anthropogenic control over gullying in the US Southwest is provide d by Cooke and Reeves (1976). Master-channel incision can be caused by vegetation degradation within the channel, for example, in the grass-covered cienega channels of the Southwest US (Melton 1965, Schumm and Hadley 1957, Bull 1997) and the Australian dambo channels (Boast 1990, Prosser and Slade 1994, Prosser et al. 1994, 1995, Rutherford et al. 1997). In this instance gully extension is just a larger example of the simulations presented here. Alternatively, incision may be due to unrelated causes such as climate change or base level change.

Erosional Processes

A variety of processes has been observed to operate at gully headwalls, including fluvial incision, seepage erosion (Howard and McLane 1988), piping (Jones 1971, 1981, Bryan and Yair 1982a, Prosser and Abernethy 1996, Fartifteh and Soeters 1999, Faulkner et al. 2000, 2007, Díaz et al. 2007), plunge-pool erosion (Stein and Julien 1993; Moore et al. 1994; Robinson and Hanson 1994, 1995, Bennett et al. 1997; Hanson et al. 1997, Stein et al. 1997: Bennett 1999, Bennett et al. 2000, Alonso et al. 2002, Bennett and Alonso 2006), and mass-wasting (Bradford et al. 1973, 1978, Blong et al. 1982; Poesen and Govers 1990: Istanbulluoglu et al. 2005; Tucker et al. 2006). General reviews are provided by Gardner (1983), Poesen and Govers (1990), Bocco (1991), Dietrich and Dunne (1993), and Bull and Kirkby (1997). The relative importance of each process varies amongst different geologic, vegetation, and climatic environments, and each process depends somewhat differently upon flow and material properties. Ephemeral gullies commonly erode by knickpoint recession of a plunge pool whereas larger gullies erode by a variety of process including plunge-pool incision, seepage erosion, piping, and mass wasting.

Predicting the initiation and temporal evolution of gully systems is difficult because of the multiplicity of processes and the threshold behaviour of gully incision. The most common approach is diagnostic rather than prognostic, assessing the spatial pattern of established gully systems. The most common approach is to examine the contributing area – slope gradient relationship at either the site of initial gullying or at its maximum extent. This approach was pioneered by Brice (1966), Patton and Schumm (1975) and Begin and Schumm (1979), put on a mechanistic foundation for a range of processes by Dietrich et al., (1992, 1993) and Montgomery and Dietrich (1994), and has been used in a number of studies of gullies (Moore et al. 1988, Vandaele et al. 1996, Vandekerckhove et al. 1998, Desmet et al. 1999, Nachtergaele et al. 2001, Morgan and Mngomezulu 2003, Poesen et al. 2003, Beechie et al. 2007, Gabet and Bookter 2007). The observed relationships between gradient and contributing area at gully heads are generally consistent with control by a shear stress threshold (e.g. Eqn. 10.8).

Gully Models

A variety of models has been used to predict the rate of gully erosion utilizing a wide range of approaches. A representative model is the Ephemeral Gully Erosion Model (EGEM) (Woodward 1999) which uses a detachment capacity proportional to applied shear stress (Equation 10.7) and a net detachment rate decreasing as sediment transport rate approaches capacity (Equation 10.6). A hydrological flow routing model is also utilized. Other theoretical approaches to gully erosion are presented by Kirkby and Bull (2000a), Casalí et al. (2003), Kirkby et al. (2003), Torri and Borselli (2003) and Sidorchuk (2005). Nachtergaele et al. (2001) and Capra et al. (2005) applied the EGEM model to a field example of ephemeral gully erosion, but found that the model had limited predictive capability, presumably due to difficulties in adequately characterizing the values of input parameters required by the model. Poesen et al. (2003, 2006) provides a comprehensive review of gully modeling approaches ranging between empirical and theoretical, concluding that extant theoretical models lack validation and calibration. Empirical models, however, while performing better for specific settings, cannot be extrapolated.

Simulating Gully Evolution

Most of the theoretical models discussed above target the evolution of individual gullies and lack the capability of predicting their areal distribution. Only a few models have attempted to explicitly model the spatial development of gullies, including Howard (1999), Kirkby and Bull (2000a), and Istanbulluoglu et al. (2005). At their present stage of development, such models are exploratory rather than useful predictive tools, but they are useful in understanding the important controls on gully development. A brief summary of the Howard (1999) model is presented here.

The Howard (1999) model assumes that erosion rates due to the dominant processes correlate with shear stress (Equation 10.7) or alternatively with drainage area and gradient (Equation 10.8). Often seepage, piping, mass wasting and plunge-pool erosion at headwalls depend upon relief generated by channel incision occurring downstream from the headwall, and therefore indirectly upon the shear stress or stream power. Where seepage erosion dominates, however, drainage area may not be a good measure of subsurface discharge (Coelho Netto and Fernandes 1990).

When the vegetation is undisturbed the critical shear stress, τ_c (Eqn. 10.7), is assumed to be areally and temporally constant. However, the critical shear stress is assumed to also depend upon the rate of erosion in a threshold manner. This critical shear stress is assumed to have a high value, τ_{cu}, so long as the local erosion rate, E (or $-\frac{\partial y}{\partial t}$), is lower than a critical value, E_u. However, if erosion locally exceeds this rate, the critical shear stress drops to a lower value, τ_{cd}, until the erosion rate drops to a low value E_d, when it is assumed that the vegetation is able to become reestablished and the critical shear stress is reestablished at the undisturbed value, τ_{cu}. In addition, the intrinsic erodibility, K_c, may increase for bare (K_{cd}) versus vegetated land surface (K_{cu}). When the erosion rate is governed by the disturbed critical shear stress, the specific runoff yield is assumed to be greater by a factor R than that of the undisturbed landscape, due to the reduction in infiltration capacity that accompanies vegetation disturbance; enhanced runoff rates from sites of vegeta-

tion disturbance or removal has been noted in several studies (Graf 1979; Prosser and Slade 1994; Parsons et al. 1996; Bull 1997). Thus, two erosional states are possible at each location in the landscape, normal and accelerated (Fig. 10.23). As is illustrated in this figure, there may be a range of steady-state erosion rates, E_n, with ($E_d < E_n < E_u$), such that the whole landscape might be in either the normal or the accelerated state depending upon the initial conditions.

Direct experimental measurements on undisturbed grasslands suggests values of critical shear stress of about 100–240 Pascals (Newtons/m^2) for undisturbed grasslands, dropping to about 70 Pascals for heavily disturbed vegetation (Reid 1989; Prosser and Slade 1994; Prosser and Dietrich 1995; Prosser et al. 1995). Bare soils have a critical shear stress of only about 0–40 Pascals (Prosser et al. 1995, Reid 1989, Knapen et al. 2007), suggesting that the ratio of τ_{cu}/τ_{cd} ranges upwards from 3 to 10 or more. Additionally, increase in vegetation density appears to decrease the erodibility coefficient, K_c, in Equation (10.7) (De Baets et al. 2006).

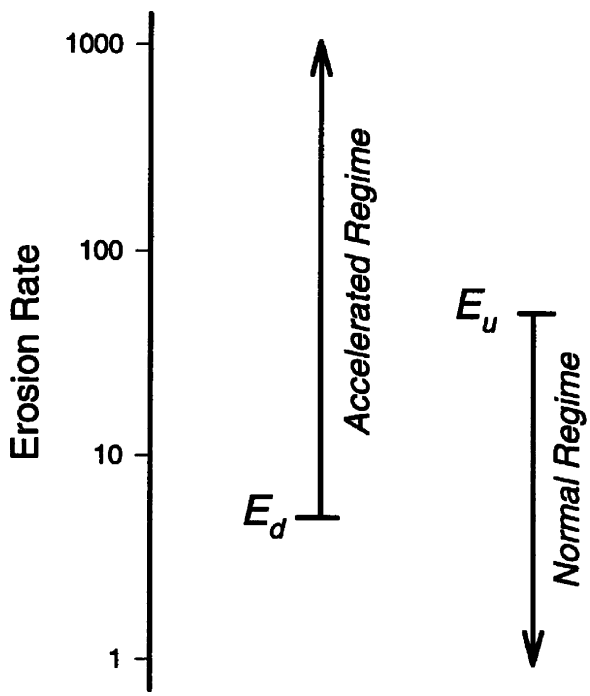

Fig. 10.23 Conceptual diagram of the limits of stability of the normal and accelerated erosional regimes in gullied landscapes. Units for erosion rates are arbitrary and the transition erosion rates E_u and E_d are discussed in the text

The initial conditions for the simulations assume that erosion has been operating in the undisturbed state and that the landscape is in steady state adjustment to an erosion rate E_n ($E_n < E_d < E_u$) with a critical shear stress τ_{cu} (e.g., broadly rounded slopes and shallow hollows in Fig. 10.24). A short-lived disturbance of the vegetation cover is assumed to occur due, perhaps, to fire, cultivation, or overgrazing. The duration of this disturbance, T_d, is assumed to be very short compared with the timescale for development of the steady state landscape, T_e. During the disturbance interval the critical shear stress is assumed to drop to a value, τ_{cx} that is less than τ_{cu} but may be greater or lesser than τ_{cd}. Following this period of disturbance the vegetation is assumed to recover, so that the critical shear stress returns to its undisturbed value, τ_{cu}, except for those portions of the landscape where $E > E_u$. In the disturbed areas fluvial erosion is governed by the parameters values τ_{cd} and K_{td}, until the erosion rate should drop to a value $E < E_d$, whereupon the undisturbed values τ_{cu} and K_{tu} are reestablished.

A short-duration lowering of the critical shear stress for fluvial erosion may be sufficient to trigger accelerated erosion in landscapes with highly erodible regolith sandwiched between a resistant vegetation cover and bedrock. The accelerated erosion may continue over periods many times the duration of the initial disturbance. Incision rates are greatest on steep hillslopes and in hollows and low-order valleys (Fig. 10.24a), whereas divides and upper slopes may revert to normal erosion rates after the short duration of vegetational stress. Erosion in high-order valleys is limited by base level control. The locus of maximum erosion gradually works headward as a shock front and eventually may consume the divide areas, even though the disturbance initiating accelerated erosion might have lasted only a short while. If the vegetation undergoes no additional disturbance, erosion will eventually reduce gradients to the point that erosion rates will revert to the normal state. A different fate may occur if the regolith is thin, because bedrock will be exposed, and reversion to the previous state of thick regolith protected by vegetation would be difficult.

The proportion of the landscape which is triggered into accelerated erosion depends upon: (1) how much the erosion resistance offered by the vegetation cover is temporarily reduced (the ratio τ_{cx}/τ_{cu} in the model); (2) the relative shearing resistance and intrinsic erodibility of the regolith compared to the vegetated surface

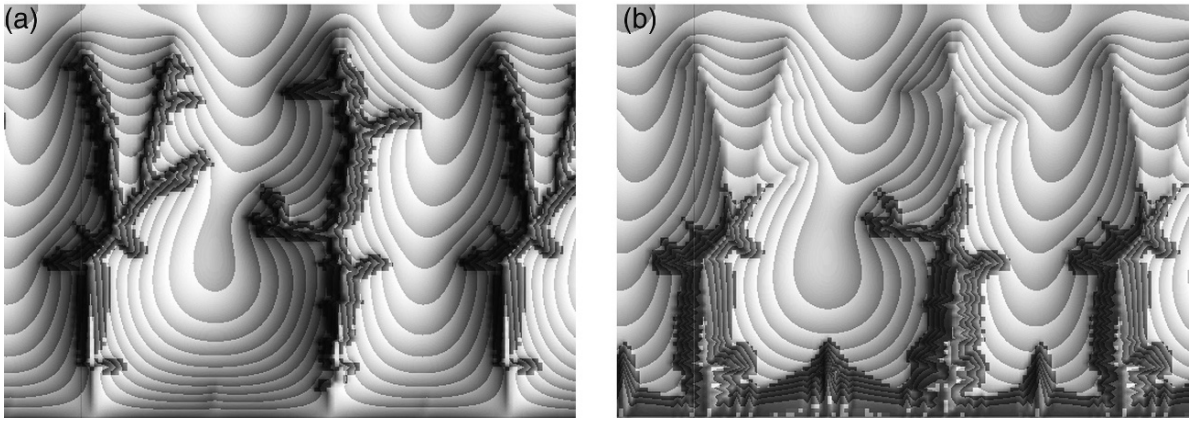

Fig. 10.24 Simulated gullying of vegetated landscape (based on Howard 1999). Boundary conditions as in Fig. 10.21. Smooth, rounded slopes and channelways are vegetated, darker areas with closely spaced contours are gullies. (**a**) Gullies developed as a result of incision through vegetation into underlying easily-eroded regolith or shale. (**b**) Gullies developed as a result of rapid downcutting of the master drainage along the lower boundary

(τ_{cd}/τ_{cu} and K_{td}/K_{tu}); (3) the rate of induced erosion which assures that the vegetation cannot become reestablished by recovery of the normal vegetation (E_u); (4) the erosion rate at which vegetation recovery is assured following the cessation of disturbance (E_d); and 5) the degree to which specific runoff is enhanced in areas with disturbed vegetation (R).

The model also illustrates the two major approaches to controlling accelerated erosion: (1) enhancement of the vegetation cover growth potential to reduce E_d, reduce runoff (R), and increase E_u; and (2) protection of the surface to increase erosional resistance (increase τ_c). Because steep, rapidly-eroding erosional fronts are created by the initial disturbance, uplands are progressively consumed by the advancing headwall even though the vegetation cover may be fully recovered. Thus structural treatments in the gullies (grade control structures, bank stabilization, etc.) are commonly required to halt their advance.

The model simulations clearly suggest that, once initiated, gullying in thick, erodible regolith or weak rocks may continue until all slopes are consumed by the wave of dissection if there is no intervention. In some environments, such unconstrained gullying and badland development may gradually consume the undisturbed areas. One well-known example is the badlands of South Dakota, which originated due to downcutting by the White River through Cenozoic shale and mudstone. These badlands have gradually advanced over thousands of years as a steep erosional front consuming a rolling, grassy upland (Fig. 10.25). Dissection of the loess terrain of China has continued over a similar timespan (Zhu Xianmo 1986). Gradual encroachment of gullies and badlands into vegetated slopes has continued over hundreds of years in Spain and Italy. In light of such examples, Bocco (1991) and Hudson (1985) suggest that gullying is not self-healing. On the other hand, inactive, naturally revegetated gullies can be found in many environments, such as the coastal ranges of California (Fig. 10.26). Graf (1977) suggests that the rate of gully extension follows a negative exponential function, decreasing to zero as the gully approaches an equilibrium length, and Graf (1977), Prosser and Abernethy (1996), and Rutherford et al. (1997) present supporting data. This equilibrium length occurs when contributing area and slope drop below threshold values (e.g., Equation 10.8).

Gullying can also be initiated by a rapid incision of the master drainage, resulting in headward knickpoint migration (Fig. 10.24b), resulting in a pattern of incision radiating from the master drainage channels.

Gullying clearly ceases in many landscapes before the entire landscape is consumed. An example is shown in Fig. 10.26. The steep, grassy landscape in the northern California Coast Ranges shown in Fig. 10.26a has been dissected by two gullies occupying colluvial hollows. The gullying may have been initiated by vege-

Fig. 10.25 An advancing erosional front in the Badlands of South Dakota, USA. Remnants of the gently-rolling grassy upland surface are visible. The gullying was triggered by late Pleistocene downcutting of the master drainage, possibly aided by a drier Holocene climate that has reduced vegetation cover. As the upland is consumed by the narrow zone of advancing badland slopes, an alluvial surface develops and extends headward. The alluvial surface in turn becomes vegetated and stabilized. In some locations additional master stream downcutting has caused dissection of the alluvial surfaces as a second erosional front. (photo by A. Howard)

tation disturbance or small landslides in the colluvial fill. The left gully in Fig. 10.26a is undergoing active extension (Fig. 10.26b), whereas the right gully (which is probably older) has become stabilized by vegetation (Fig. 10.26c). The factors leading to the restabilization are uncertain, but may include diminished incision rates when incision of the main channel reached bedrock, the greater moisture supply in the gully floor encouraging vegetation regrowth, and wet seasons with abundant moisture but no strong storms.

Several circumstances can encourage gully stabilization. Headward erosion of gullies in the landscape studied by Prosser and Abernethy (1996) cease when the gullies incised into alluvium reach the base of the hillslopes, which are shallowly underlain by bedrock. Exposure of bedrock may prevent plunge-pool erosion and enhance revegetation by reducing erosion rates in valley bottoms and encouraging seepage discharge along gully walls.

The simple Howard (1999) model assumes spatially and temporally invariant erosion rate thresholds and spatially invariant critical shear stress. Spatial variation may occur in both erosion thresholds and critical shear stress. In semi-arid landscapes vegetation density and growth rates may be greatest in hollows and valley bottoms. As a result, the critical shear stress, (τ_c), may be higher in valleys as might be the erosion rate, E_u required to initiate gully development. In some circumstances, gullies might develop on convex hillslopes while hollows and valleys remain stable despite their greater source drainage area. Gully incision also may increase the delivery of moisture to headwalls by groundwater seepage or baseflow, thus encouraging revegetation due to a higher erosion rate reversion to normal condition, E_d, not accounted for in the present model. This erosion rate transition, E_d, may also be time-dependent, increasing during wet periods. Revegetation can also be encouraged during periods of low erosion rates in intervals lacking major storm runoff. Finally, supply of subsurface water to headwalls extended by groundwater seepage may drop to zero as the channels become less incised upon reaching the upper portions of hollows and sideslopes.

A more elaborate treatment of precipitation forcing and vegetative growth is presented by Istanbulluoglu et al. (2005) and Tucker et al. (2006) involving simulation of individual precipitation events and vegetative growth and disturbance dynamics. High intensity rains encourage incision by increasing the applied shear stress (high values of K_c in Equation 10.7). Frequent

low intensity events encourage vegetation growth by increasing τ_c, E_u, and E_d, whereas droughts would have the opposite effect.

Some landscapes may experience natural epicycles of gully erosion without external forcing, possibly analogous to the cycles of colluvial infilling and landslide excavation in hollows in steep landscapes of the Pacific Rim (Dietrich and Dunne 1978, Reneau and Dietrich 1991, Benda and Dunne 1997). In fact, the partial excavation of hollows by landslides can trigger further incision by gully extension. Such a mechanism might have triggered the gullies shown in Figs. 10.22 and 10.26. Landsliding may not be a necessary trigger, however, because colluvial infilling of hollows may provide a sufficient imbalance. Colluvial filling decreases the concavity of hollows, which increases gradients at the base of the hollow where contributing drainage area is the greatest, so that shear stresses are increased. In addition, the decreased concavity may reduce available moisture and thus decrease the vegetation density.

A similar approach can be utilized to predict entrenchment in larger vegetated streams or unchanneled valleys, such as in cienegas (Leopold and Miller 1956, Melton 1965, Bull 1997) and dambos (Boast 1990, Prosser and Slade 1994, Prosser et al. 1994). If channels have modest maximum flow intensities and a high frequency of low flows, vegetation (often grasses and sedges) may cover the channel bed. This reduces shear stresses on the bed and encourages sedimentation. However, as with the gullying discussed above, rapid incision into the vegetation cover can occur due to either high flow intensities or reduced vegetation density following droughts. This leads to a tendency for valley

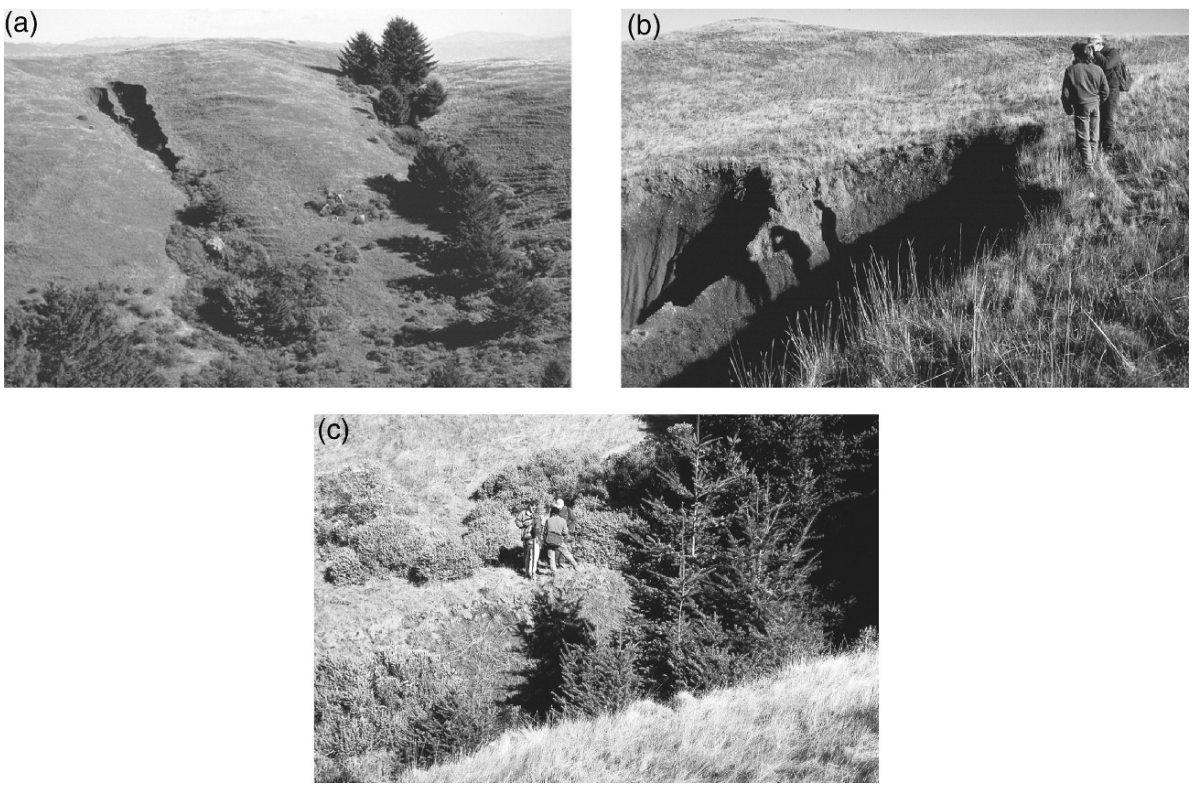

Fig. 10.26 Stable and active gullies in the coastal hills north of San Francisco, California, USA. (**a**) The left gully is actively extending headwards, whereas the right gully has become stablilized. Both gully systems occupy colluvial hollows. (**b**) View looking across the head of the left gully in (**a**). Note the abrupt headwall, the steep slopes undergoing rapid mass wasting, and the high drainage density on the headwall. Headwall retreat occurs both by runoff and shallow slumping as well as deeper rotational slumps. (**c**) View across the right gully in (**a**), showing the high vegetation density in the hollow, which has inhibited downcutting and promoted revegetation of the headwalls. Some localized headwall retreat is still occurring, as below and to the left of the figures. The causes for the contrast between the two gully systems is discussed in the text. (photos by A. Howard)

bottoms to alternate between periods of aggradation when flows are broad and shallow through abundant vegetation versus cycles of entrenchment in narrow, unvegetated incised channels. Autogenic cycles of incision and aggradation influenced by vegetation may alternate not only temporally, but spatially as well in the guise of discontinuous gullies (Schumm and Hadley 1957, Leopold and Miller 1956, Blong 1970, Bull 1997).

Conclusions

Despite the apparent morphologic simplicity of badland and gully systems and the similarity in features over a wide range of environments and lithology, the formative processes are surprisingly diverse and remain difficult to quantify. For example, runoff and erosion of badland slopes involves a complex combination of runoff, infiltration through cracks, flow in macropores, clay swelling and dispersion, chemical leaching, and a strong dependence of these processes on precipitation history. Similarly, erosion of gully heads may occur through vegetation disturbance, plunge pool scour, mass wasting, seepage erosion, and piping. Further understanding of badlands will require studies conducted at a range of temporal and spatial scales. Approaches include unraveling the erosional history, runoff plot experiments conducted either in the field regolith or laboratory, study of weathering processes and regolith structure, and development of mathematical models. Badlands and gully systems offer a unique opportunity for development and testing of quantitative landform models, because we not only have the landform morphology to compare with theoretical models, but processes are rapid enough that rates of landform change can be measured with reasonable accuracy over periods of just a few years.

References

Ahnert, F. 1976. Brief description of a comprehensive three-dimensional process-response model of landform development. *Zeitschrift für Geomorphologie Supplement Band* **25**, 29–49.

Ahnert, F. 1977. Some comments on the quantitative formulation of geomorphological processes in a theoretical model. *Earth Surface Processes* **2**, 191–202.

Ahnert, F. 1987a. Approaches to dynamic equilibrium in theoretical simulations of slope development. *Earth Surface Processes and Landforms* **12**, 3–15.

Ahnert, F. 1987b. Process-response models of denudation at different spatial scales. *Catena Supplement* **10**, 31–50.

Ahnert, F. 1988. Modelling landform change. In *Modelling Geomorphological Processes*, M.G. Anderson (Ed.), 375–400. Chichester: John Wiley & Sons.

Akky, M.R. and Shen, C. K. 1973. Erodibility of a cement-stabilized sandy soil. In *Soil erosion: causes and mechanisms*. U.S. Highway Research Board Special Report 135, 30–41.

Alexander, R., Harvey, A. M., Calvo, A., James, P. A. and Cerda, A. 1994, Natural stabilization mechanisms on badland slopes, Tibernas, Almeria, Spain. In *Environmental Change in Drylands: Biogeographical and Geomorphological Perspectives*, Millington, A.C. and Pye, K. (Eds), 85–111, Wiley, Chichester.

Alonso, C., Bennett, S.J. and Stein, O.R. 2002. Predicting head cut erosion and migration in concentrated flows typical of upland areas. *Water Resources Research* **38**, doi:10.1029/2001WR001173.

Anderson, R. S., Repka, J. L. and Dick, G. S., 1996. Explicit treatment of inheritance in dating depositional surfaces using in situ ^{10}Be and ^{26}Al, *Geology* **24**, 47–51.

Ariathurai, R. and Arulandan, K. 1986. Erosion rates of cohesive soils. *Journal of the Hydraulics Division, American Society of Civil Engineers* **104**, 279–298.

Battaglia, S., Leoni, L. and Sartori, F. 2002. Mineralogical and grain size composition of clays developing calanchi and biancane erosional landforms. *Geomorphology* **49**, 153–170.

Beechie, T.J., Pollock, M.M. and Baker, S. 2007. Channel incision, evolution and potential recovery in the Walla Walla and Tucannon River basins, northwestern USA. *Earth Surface Processes and Landforms*, doi: 10.1002/esp.1578.

Begin, Z.B. and Schumm, S.A. 1979. Instability of alluvial valley floors: A method for its assessment, *Transactions of the American Society of Agricultural Engineers* **22**, 347–350.

Benda, L. and Dunne, T. 1997. Stochastic forcing of sediment supply to channel networks from landsliding and debris flow, *Water Resources Research* **33**, 2849–2863.

Bennett, S.J. 1999. Effect of slope on the growth and migration of headcuts in rills. *Geomorphology* **30**, 273–290.

Bennett, S.J., Alonso, C., Prasad, S.N. and Römkens, M.J.M. 2000. A morphological study of headcut growth and migration in upland concentrated flows. *Water Resources Research* **36**, 1911–1922.

Bennett, S.J. and Alonso, C.V. 2006. Turbulent flow and bed pressure within headcut scour holes due to plane reattached jets. *Journal of Hydraulic Research* **44**, 510–521.

Bennett, S.J., Alonso, C.V., Prasad, S.N. and Römkens, M.J.M. 1997. Dynamics of head-cuts in upland concentrated flows. In *Management of landscapes disturbed by channel incision*, Wang, S.Y., Langendoen, E.J. and Shields, F.D. Jr. (Eds.), 510–515, University of Mississippi, Oxford, Miss.

Biot, Y. 1990. THEPROM – an erosion productivity model. In *Soil erosion on agricultural land*, Boardman, J., Foster, I.D.L. and Dearing, J.A. (Eds), 465–479, John Wiley & Sons, Chichester.

Blong, R.J. 1970. The development of discontinuous gullies in a pumice catchment. *American Journal of Science* **268**, 369–384.

Blong, R.J., Graham, O.P. and Veness, J.A. 1982. The role of sidewall processes in gully development; some N.S.W. examples. *Earth Surface Processes and Landforms* **7**, 381–385.

Boast, R. 1990. Dambos: A review. *Progress in Physical Geography* **14**, 153–177.

Bocco, G. 1991. Gully erosion: processes and models. *Progress in Physical Geography* **15**, 392–406.

Bouma, N.A. and Imeson, A.C. 2000. Investigation of relationships between measured field indicators and erosion processes on badland surfaces at Petrer, Spain. *Catena* **40**, 141–171.

Bowyer-Bower, T.A.S. and Bryan, R. B. 1986. Rill initiation: concepts and evaluation on badland slopes. *Zeitschrift für Geomorphologie Supplement Band* **59**, 161–175.

Bradford, J.M., Farrell, D.A. and Larson, W.W. 1973. Mathematical evaluation of factors affecting gully stability. *Soil Science Society American Proc.*, **37**, 103–107.

Bradford, J.M., Piest, R.F. and Spomer, R.G. 1978. Failure sequence of gully headwalls in western Iowa. *Soil Science Society of America Journal* **42**, 323–238.

Bradley, W.H. 1940. Pediments and pedestals in miniature. *Journal of Geomorphology* **3**, 244–554.

Brice, J.C. 1966. Erosion and deposition in the loess-mantled Great Plains, Medicine Creek drainage basin, Nebraska. *U. S. Geological Survey Professional Paper 352H*, 255–335.

Bryan, R.B. 1987. Processes and significance of rill development. *Catena Supplement* **8**, 1–15.

Bryan, R.B., Campbell, I.A. and Yair, A. 1987. Postglacial geomorphic development of the Dinosaur Provincial Park badlands, Alberta. *Canadian Journal of Earth Sciences* **24**, 135–146.

Bryan, R.B., Imeson A.C. and Campbell, I.A. 1984. Solute release and sediment entrainment on microcatchments in the Dinosaur Park badlands, Alberta Canada. *Journal of Hydrology* **71**, 79–106.

Bryan, R. and Yair, A. 1982a. Perspectives on studies of badland geomorphology. In *Badland Geomorphology and Piping*, Bryan, R. B. and Yair, A. (eds), 1–13. Norwich: Geo Books, Norwich, England.

Bryan, R. and Yair, A. (eds). 1982b. *Badland geomorphology and piping*. Norwich: Geo Books.

Bryan, R.B., Yair, A. and Hodges, W. K. 1978. Factors controlling the initiation of runoff and piping in Dinosaur Provincial Park badlands, Alberta, Canada. *Zeitschrift für Geomorphologie Supplement Band* **34**, 48–62.

Bull, L.J. and Kirkby, M.J. 1997. Gully processes and modelling. *Progress in Physical Geography* **21**, 354–374.

Bull, W.B. 1997. Discontinuous ephemeral streams. *Geomorphology* **19**, 227–276.

Campbell, I.A. 1989. Badlands and badland gullies. In *Arid Zone Geomorphology*, Thomas, D.S.G. (ed), 159–193. New York: Halstead Press.

Campbell, I.A. and Honsaker, J. L. 1982. Variability in badlands erosion; problems of scale and threshold identification. In *Space and Time in Geomorphology*, Thorn, C. E. (ed), 59–79. London: George Allen & Unwin.

Capra, A., Mazzara, L.M. and Scicolone, B. 2005. Application of the EGEM model to predict ephemeral gully erosion in Sicily, Italy. *Catena* **59**, 133–146.

Carman, M.F., Jr. 1958. Formation of badland topography. *Geological Society of America Bulletin* **69**, 789–790.

Carson, M.A. 1969. Models of hillslope development under mass failure. *Geographical Analysis* **1**, 76–100.

Carson, M.A. 1971. An application of the concept of threshold slopes to the Laramie Mountains, Wyoming. *Institute of British Geographers Special Publication* **3**, 31–47.

Carson, M.A. and Kirkby, M. J. 1972. *Hillslope form and Process*, 475pp. Cambridge: Cambridge University Press.

Carson, M.A. and Petley, D. J. 1970. The existence of threshold slopes in the denudation of the landscape. *Transactions of the Institute of British Geographers* **49**, 71–95.

Casalí, J., López, J.J. and Giráldez, J.V. 2003. A process-based model for channel degradation: application to ephemeral gully erosion. *Catena* **50**, 435–447.

Cerdà, A. and García Fayos, P. 1997. The influence of slope angle on sediment, water and seed losses on badland landscapes. *Geomorphology* **18**. 77–90.

Chisci, G., Sfalanga, M. and Torri, D. 1985. An experimental model for evaluating soil erosion on a single-rainstorm basis. In *Soil Erosion and Conservation*, Swaify, S. A., Moldenhauer, W. C. and Lo, A. (eds), 558–565. Ankeny, Iowa: Soil Conservation Society of America.

Churchill, R.R. 1981. Aspect-related differences in badlands slope morphology. *Annals of the Association of American Geographers* **71**, 374–388.

Coelho Netto, A.L. and Fernandes, N.F. 1990. Hillslope erosion, sedimentation, and relief inversion in SW Brazil: Bananal, SP. *International Association of Scientific Hydrology Publication* **192**, 174–182.

Collins, D.B.G., Bras, R.L. and Tucker, G.E. 2004. Modeling the effects of vegetation-erosion coupling on landscape evolution. *Journal of Geophysical Research* **109**, F03004, doi:10.1029/2003JF000028.

Cooke, R.U. and Reeves, W.R.1976. *Arroyos and Environmental Change in the American South-West*, Clarendon Press, Oxford.

Coulthard, T.J. 2001. Landscape evolution models: a software review. *Hydrological Processes* **15**, 165–173.

Coulthard, T.J., Kirkby, M.J. and Macklin, M.G. 2000. Modelling geomorphic response to environmental change in an upland catchment. *Hydrological Processes* **14**, 2031–2045.

Coulthard, T.J., Macklin, M.G. and Kirkby, M.J. 2002. A cellular model of Holocene upland river basin and alluvial fan evolution. *Earth Surface Processes and Landforms* **27**, 269–288.

Culling, W.E.H. 1963. Soil creep and the development of hillside slopes. *Journal of Geology* **71**, 127–161.

Daniels, R.B. 1960. Entrenchment of the Willow Drainage Ditch, Harrison County, Iowa. *American Journal of Science* **258**, 161–176.

Daniels, R.B. and Jordan, R.H. 1966. Physiographic history and the soils, entrenched stream systems and gullies, Harrison County, Iowa. *U.S. Department of Agriculture Technical Bulletin* **1348.**

Darby, S.E. and Simon, A. (eds). 1999. *Incised River Channels: Processes, forms, Engineering and Management*. Wiley, Chichester, 442pp.

Davis, W.M. 1892. The convex profile of bad-land divides. *Science* **20**, 245.

De Baets, S., Poesen, J., Gyssels, G. and Knapen, A. 2006. Effects of grass roots on the erodibility of topsoils during concentrated flow. *Geomorphology* **76**, 54–67.

Desir, G. and Marín, C. 2006. Factors controlling the erosion rates in a semi-arid zone (Bardenas Reales, NE Spain). *Catena*, doi:10.1016/j.catena.2006.10.004.

Desmet, P.J.J., Poesen, J., Govers, G. and Vandaele, K. 1999. Importance of slope gradient and contributing area for optimal prediction of the initation and trajectory of ephemeral gullies. *Catena* **37**, 377–392.

Díaz, A.R., Sanleandro, P.M., Soriano, A.S., Serrato, F.B. and Faulkner, H. 2007. The causes of piping in a set of abandoned agricultural terraces in southeast Spain. *Catena* **69**, 282–293.

Dietrich, W.E. and Dunne, T. 1978. Sediment budget for a small catchment in mountainous terrain. *Zeitschrift für Geomorphology Supplement* **29**, 191–206.

Dietrich, W.F. and Dunne, T. 1993. The channel head, In *Channel network hydrology*, Beven, K. and Kirkby, M.J. (eds), 175–219, Wiley, Chichester.

Dietrich, W.F., Wilson, C.J, Montgomery, D.R., McKean, J. and Bauer, R. 1992. Erosion threshold and land surface morphology. *Geology* **20**, 675–679.

Dietrich, W.E., Wilson, C.J., Montgomery, D.R., McKean, J. 1993. Analysis of erosion thresholds, channel networks, and landscape morphology using a digital terrain model, *Journal of Geology* **101**. 259–278.

Dunne, T. and Aubrey, B.F. 1986. Evaluation of Horton's theory of sheetwash and rill erosion on the basis of field experiments. In *Hillslope Processes*, Abrahams, A. D. (ed), 31–53. Boston: Allen & Unwin.

Emmett, W.W. 1970. The hydraulics of overland flow on hillslopes. *U.S. Geological Survey Professional Paper* 662-A.

Engelen, G.B. 1973. Runoff processes and slope development in Badlands National Monument, South Dakota. *Journal of Hydrology* **18**, 55–79.

Everaert, W. 1991. Empirical relations for the sediment transport capacity of interrill flow. *Earth Surface Processes and Landforms* **16**, 513–532.

Fagherazzi, S., Howard, A.D. and Wiberg, P.L. 2004. Modeling fluvial erosion and depositon on continental shelves during sea level cycles. *Journal of Geophysical Research* **109**, F03010, doi:10.1029/2003JF000091.

Fartifteh, J. and Soeters, R. 1999. Factors underlying piping in the Basilicata region, southern Italy. *Geomorphology* **26**, 239–251.

Faulkner, H., Alexander, R. and Wilson, B.R. 2003. Changes to the dispersive characteristics of soils along an evolutionary slope sequence in the Vera badlands, southeast Spain: implications for site stabilisation. *Catena* **50**, 243–254.

Faulkner, H., Alexander, R. and Zukowskyj, P. 2007. Slope-channel coupling between pipes, gullies and tributary channels in the Mocatán catchment badlands, Southeast Spain. *Earth Surface Processes and Landforms*, doi: 10.1002/esp. 1610.

Faulkner, H., Sípivey, D. and Alexander, R. 2000. The role of some site geochemical processes in the development and stabilisation of three badland sites in Almería, Southern Spain. *Geomorphology* **35**, 87–99.

Fernandes, N.F. and Dietrich, W.E. 1997. Hillslope evolution by diffusive processes: the timescale for equilibrium adjustments, *Water Resources Research* **33**, 1307–1318.

Finlayson, B.L., Gerits, J. and van Wesemael, B. 1987. Crusted microtopography on badland slopes in southeast Spain. *Catena* **14**, 131–144.

Foster, G.R. 1982. Modeling the erosion process. In *Hydrologic Modeling of Small Watersheds*, C.T. Hahn, H.P. Johnson and Brakensiek, D. L. (eds), 297–382. St. Joseph, Michigan: American Society of Agricultural Engineers.

Foster, G.R. 1990. Process-based modelling of soil erosion by water on agricultural land. In *Soil Erosion on Agricultural Land*, Boardman, J., Foster, I. D. L. and Dearing, J. A. (eds), 429–445. Chichester: John Wiley & Sons.

Foster, G.R. and Lane, L.J. 1983. Erosion by concentrated flow in farm fields. In *Proceedings of the D.B. Simons Symposium on Erosion and Sedimentation, 9.65–9.82*. Fort Collins, Colorado: Colorado State University.

Foster, G.R. and Meyer, L.D. 1972. A closed-form soil erosion equation for upland areas. I*n Sedimentation (Einstein)*, Shen, H.W. (ed), 12,1–12,19. Fort Collins, Colorado: Colorado State University.

Gabet, E.J. and Bookter, A. 2007. A morphometric analysis of gullies scoured by post-fire progressively bulked debris flows in southwest Montana, USA. *Geomorphology*, doi:10.1016/j.geomorph.2007.03.016.

Garcia-Castellanos, D. 2002. Interplay between lithospheric flixure and river transport in foreland basins. *Basin Research* **14**, 89–104.

Gardner, T.W. 1983. Experimental study of knickpoint migration and longitudinal profile evolution in cohesive, homogeneous material. *Geological Society of America Bulletin* **94**, 664–672.

Gasparini, N.M., Whipple, K.X. and Bras, R.L. 2007. Predictions of steady state and transient landscape morphology using sediment-flux-dependent river incision models. *Journal of Geophysical Research* **112**, F03S09, doi:10.1029/2006JF000567.

Gerits, J., Imeson, A.C., Verstraten, J.M. and Bryan, R. B. 1987. Rill development and badland regolith properties. *Catena Supplement* **8**, 141–160.

Gilbert, G.K. 1880. *Report on the Geology of the Henry Mountains.* Washington: U.S. Geographical and Geological Survey of the Rocky Mountain Region.

Gilbert, G.K. 1909. The convexity of hilltops. *Journal of Geology* **17**, 344–351.

Gilley, J.E., Woolhiser, D.A. and McWhorter, D. B. 1985. Interrill soil erosion – Part I: Development of model equations. *Transactions of the American Society of Agricultural Engineers* **28**, 147–153, 159.

Govers, G. 1985. Selectivity and transport capacity of thin flows in relation to rill erosion. *Catena* **12**, 35–49.

Govers, G. and Rauws, G. 1986. Transporting capacity of overland flow on plane and on irregular beds. *Earth Surface Processes and Landforms* **11**, 515–524.

Graf, W.L. 1977. The rate law in fluvial geomorphology. *American Journal of Science* **277**, 178–191.

Graf, W.L. 1979. The development of montane arroyos and gullies. *Earth Surface Processes* **4**, 1–14.

Guy, H.P. 1965. Residential construction and sedimentation at Kensington, Maryland. In *Federal Inter-Agency Sedimentation Conference Proceedings 1963*, U.S. Department of Agriculture Miscellaneous Publication **970**, 30–37.

Guy, H.P. 1972. Urban sedimentation – in perspective. *Proceedings of the American Society of Civil Engineers, Journal of the Hydraulics Division* **98**, 2009–2016.

Hanson, G.J., Robinson, K.M. and Cook, K.R.1997. Experimental flume study of headcut migration. In *Management of Landscapes Disturbed by Channel Incision*, Wang, S.Y., Langendoen, E.J. and Shields, F.D. Jr. (eds.), 503–509, Oxford, Miss: University of Mississippi.

Happ, S.C. Rittenhouse, G. and Dobson, G.C. 1940. Some principles of accelerated stream and valley sedimentation. *U.S. Department of Agriculture Technical Bulletin* **695**, 133pp.

Harvey, A. 1982. The role of piping in the development of badlands and gully systems in south-east Spain. In *Badland Geomorphology and Piping*, Bryan, R. and Yair, A. (eds), 317–335. Norwich: Geo Books.

Harvey, A.M. 1992. Process interactions, temporal scales and the development of hillslope gully systems: Howgill Fells, northwest England, *Geomorphology*, **5**, 323–344.

Hirano, M. 1975. Simulation of developmental process of interfluvial slopes with reference to graded form. *Journal of Geology* **83**, 113–123.

Hodges, W.K. 1982. Hydraulic characteristics of a badland psuedo-pediment slope system during simulated rainstorm experiments. In *Badland Geomorphology and Piping*, Bryan, R. and Yair, A. (eds), 127–151. Norwich: Geo Books.

Hodges, W.K. and Bryan, R.B. 1982. The influence of material behavior on runoff initiation in the Dinosaur Badlands, Canada. In *Badland Geomorphology and Piping*, Bryan, R. and Yair, A. (eds), 13–46. Norwich: Geo Books.

Howard, A. D. 1970. A study of process and history in desert landforms near the Henry Mountains, Utah. Unpublished PhD dissertation, 198pp. Baltimore: Johns Hopkins University.

Howard, A.D. 1980. Thresholds in river regime. In *Thresholds in Geomorphology*, Coates, D. R. and Vitek, J. D. (eds), 227–258. London: George Allen & Unwin.

Howard, A.D. 1982. Equilibrium and time scales in geomorphology: application to sand-bed alluvial channels. *Earth Surface Processes and Landforms* **7**, 303–325.

Howard, A. D. 1994a. Badlands. In *Geomorphology of Desert Environments*, Abrahams, A. D. and Parsons, A. J. (eds), 213–242. London: Chapman & Hall.

Howard, A. D. 1994b. A detachment-limited model of drainage basin evolution. *Water Resources Research* **30**, 2261–2285.

Howard, A.D. 1997. Badland morphology and evolution: Interpretation using a simulation model. *Earth Surface Processes and Landforms* **22**, 211–227.

Howard, A.D. 1998. Long profile development of bedrock channels: Interaction of weathering, mass wasting, bed erosion and sediment transport. *American Geophysical Union Geophysical Monograph* **107**, 297–319.

Howard, A.D. 1999. Simulation of gully erosion and bistable landforms. In *Incised Channels*, Darby, S. and A. Simon, A. (eds), *Incised Channels*, 277–300. New York: Wiley.

Howard, A.D. 2007. Simulating the development of martian highland landscapes through the interaction of impact cratering, fluvial erosion, and variable hydrologic forcing. *Geomorphology* **91**, 332–363.

Howard, A.D. and Kerby, G. 1983. Channel changes in badlands. *Geological Society of America Bulletin* **94**, 739–752.

Howard, A.D. and McLane, C.F. 1988. Erosion of cohesionless sediment by groundwater seepage. *Water Resources Research*, **24**, 1659–1674.

Hudson, N.W. 1985. *Soil Conservation*, London: Batsford.

Hunt, C.B. 1953. Geology and Geography of the Henry Mountains Region. *U. S. Geological Survey Professional Paper* 228.

Imeson, A.C. and Verstraten, J. M. 1985. The erodibility of highly calcareous soil material from southern Spain. *Catena* **12**, 291–306.

Imeson, A.C. and Verstraten, J. M. 1988. Rills on badland slopes: a physico-chemically controlled phenomenon. *Catena Supplement* **12**, 139–150.

Imeson, A.C., Kwaad, F.J.P.M. and Verstraten, J.M. 1982. The relationship of soil physical and chemical properties to the development of badlands in Morocco. In *Badland Geomorphology and Piping*, Bryan, R. and Yair, A. (eds), 47–69. Norwich: Geo Books, Norwich.

Ireland, H.A., Sharpe, C.F.S. and Eargle, D.H. 1939. Principles of gully erosion in the Piedmont of South Carolina. *U.S. Department of Agriculture Technical Bulletin*, **633**, 143pp.

Istanbulluoglu, E. and Bras, R.L. 2005. Vegetation-modulated landscape evolution: Effects of vegetation on landscape processes, drainage density, and topography. *Journal of Geophysical Research* **110**, F02012, doi:10.1029/2004JF000249).

Istanbulluoglu, E., Bras, R.L. and Flores-Cervantes, H. 2005. Implications of bank failures and fluvial erosion for gully development: Field observations and modeling. *Journal of Geophysical Research* **110**, F01014, doi:10.1029/2004JF000145.

Jacobson, R.B. and Coleman, D.J. 1986. Stratigraphy and recent evolution of Maryland Piedmont flood plains *American Journal of Science*, **268**, 613–637.

Jones, J.A.A. 1971. Soil piping and stream channel initiation. *Water Resources Research* **7**, 602–610.

Jones, J.A.A. 1981. *The Nature of Soil Piping – A Review of Research*, British Geomorphology Research Group Monograph **3**, Geobooks, Norwich.

Jones, J.A.A. 1990. Piping effects in drylands. *Geological Society of America Special Paper* **252**, 111–138.

Julian, P.Y. and Simons, D. B. 1985. Sediment transport capacity of overland flow. *Transactions of the American Society of Agricultural Engineers* **28**, 755–762.

Karcz, I. and Kersey, D. 1980. Experimental study of free-surface flow instability and bedforms in shallow flows. *Sedimentary Geology* **27**, 263–300.

Kasanin-Grubin, M. and Bryan, R. 2007. Lithologic properties and weathering response on badland hillslopes. *Catena* **70**, 68–78.

Kinnell, P.I.A. 1990. Modelling erosion by rain-impacted flow. *Catena Supplement* **17**, 55–66.

Kinnell, P.I.A. 1991. The effect of flow depth on sediment transport induced by raindrops impacting shallow flows. *American Society of Agricultural Engineers Transactions* **34**, 161–168.

Kirkby, M.J. 1971. Hillslope process-response models based on the continuity equation. *Institute of British Geographers Special Publication* **3**, 15–30.

Kirkby, M.J. 1976a. Soil development models as a component of slope models. *Earth Surface Processes* **2**, 203–230.

Kirkby, M.J. 1976b. Deterministic continuous slope models. *Zeitschrift für Geomorphology Supplementband* **25**, 1–19.

Kirkby, M.J. 1980a. Modelling water erosion processes. In*Soil Erosion*, Kirkby, M.J. and Morgan, R.P.C. (eds), 183–216. Chichester: John Wiley & Sons.

Kirkby, M. J. 1980b. The stream head as a significant geomorphic threshold. In *Thresholds in Geomorphology*, Coates, D.R. and Vitek, J.D. (eds), 53–73. London: George Allen & Unwin.

Kirkby, M.J. 1984. Modelling cliff development in South Wales: Savigear re-viewed. *Zeitschrift für Geomorphologie* **28**, 405–426.

Kirkby, M.J. 1985a. The basis for soil profile modelling in a geomorphic context. *Journal of Soil Science* **36**, 97–122.

Kirkby, M.J. 1985b. A model for the evolution of regolith-mantled slopes. In *Models in Geomorphology*, Woldenberg, M. J. (ed), 213–237. Boston: Allen & Unwin.

Kirkby, M.J. 1986. A two-dimensional simulation model for slope and stream evolution. In *Hillslope Processes*, Abrahams, A. D. (ed), 203–222. Winchester: Allen & Unwin.

Kirkby, M.J. 1990. A one-dimensional model for rill inter-rill interactions. *Catena Supplement* **17**, 133–146.

Kirkby, M.J., Bull, L.J., Poesen, J., Nachtergaele, J. and Vandekerckhove, L. 2003. Observed and modelled distributions of channel and gully heads – with examples from SE Spain and Belgium. *Catena* **50**, 415–434.

Kirkby, M.J. and Bull, L.J. 2000a. Some factors controlling gully growth in fine-grained sediments: a model applied in southeast Spain. *Catena* **40**, 127–146.

Kirkby, M.J. and Bull, L.J. 2000b. Some factors controlling gully growth in fine-grained sediments; a model applied in Southeast Spain. In *Badlands in Changing Environments*, Torri, D., Poesen, J., Calzolari, C. and Rodolfi, G. (eds), 127–146. Catena-Verlag Rohdenburg, Cremlingen-Destedt.

Knapen, A., Poesen, J., Govers, G., Gyssels, G. and Nachtergaele, J. 2007. Resistance of soils to concentrated flow erosion: A review. *Earth-Science Reviews* **80**, 75–109.

Komura, S. 1976. Hydraulics of slope erosion by overland flow. *Journal of the Hydraulics Division, American Society of Civil Engineers* **102**, 1573–1586.

Kuhn, N.J. and Yair, A. 2004. Spatial distribution of surface conditions and runoff generation in small arid watersheds, Zin Valley Badlands, Israel. *Geomorphology* **57**, 183–200.

Kuijper, C., Cornelisse, J.M. and Winterwerp, J. C. 1989. Research on erosive properties of cohesive sediments. *Journal of Geophysical Research* **94**, 14341–14350.

Lambe, T.W. and Whitman, R.V. 1969. *Soil mechanics*, 553pp. New York: Wiley.

Lane, L.J., Shirley, E.D. and Singh, V.P. 1988. Modelling erosion on hillslopes. In *Modelling Geomorphological Systems*, M.G. Anderson (ed), 287–308. Chichester: John Wiley & Sons.

Laronne, J.B. 1981. Dissolution kinetics of Mancos Shale – associated alluvium. *Earth Surface Processes and Landforms* **6**, 541–552.

Laronne, J.B. 1982. Sediment and solute yield from Mancos Shale hillslopes, Colorado and Utah. In *Badland Geomorphology and Piping*, Bryan, R. and A. Yair, A. (eds), 181–192. Norwich: Geo Books.

Leopold, L.B. and Miller, J.P. 1956. Ephemeral streams. Hydraulic factors and their relation to the drainage net. *U.S. Geological Survey Professional Paper* **282–A**.

Mackin, J.H. 1948. Concept of the graded river. *Geological Society of America Bulletin* **59**, 463–512.

Melton, M.A. 1965. The geomorphic and paleoclimatic significance of alluvial deposits in southern Arizona, *Journal of Geology* **73**, 1–38.

Meyer, L.D. 1986. Erosion processes and sediment properties for agricultural cropland. In *Hillslope Processes*, Abrahams, A.D. (ed), 55–76. Winchester: Allen & Unwin.

Meyer L.D. and Monke, E.J. 1965. Mechanics of soil erosion by rainfall and overland flow. *Transactions of the American Society of Agricultural Engineers* **8**, 572–577, 580.

Montgomery, D.R. and Dietrich, W.E. 1994. landscape dissection and drainage area-slope thresholds. In *Process Models and Theoretical Geomorphology*, Kirkby, M.J. (ed.), 221–245, John Wiley & Sons, Chichester.

Moore, I.D., Burch, G.J. and MacKenzie, D.H. 1988. Topographic effects on the distribution of surface soil water and the location of ephemeral gullies. *Transactions American Society of Agricultural Engineers* **31**, 1098–1107.

Moore, J.S., Temple, D.M. and Kirsten, H.A.D. 1994. Headcut advance threshold in earth spillways. *Bulletin of the Association of Engineering Geology* **31**, 277–280.

Morgan, R.P.C. and Mngomezulu, D. 2003. Threshold conditions for initiation of valley-side gullies in the Middle Veld of Swaziland. *Catena* **50**, 401–414.

Moseley, M.P. 1973. Rainsplash and the convexity of badland divides. *Zeitschrift für Geomorphologie Supplementband* **18**, 10–25.

Moss, A.J., Green, P. and Hutka, J. 1982. Small channels: their experimental formation, nature and significance. *Earth Surface Processes and Landforms* **7**, 401–416.

Moss, A.J. and Walker, P.H. 1978. Particle transport by continental water flow in relation to erosion, deposition, soils and human activities. *Sedimentary Geology* **20**, 81–139.

Moss, A.J., Walker, P.H. and Hutka, J. 1979. Raindrop-stimulated transportation in shallow water flows: an experimental study. *Sedimentary Geology* **22**, 165–184.

Nachtergaele, J., Poesen, J., Steegen, A., Takken, I., Beuselinck, L., Vandekerckhove, L. and Govers, G. 2001. The value of a physically based model versus an empirical approach in the prediction of ephemeral gully erosion for loess-derived soils. *Geomorphology*, **40** , 237–252.

Nadal-Romero, E., Regüés, D., Martí-Bono, C. and Serrano-Muela, P. 2007. Badland dynamics in the Central Pyrenees: temporal and spatial patterns of weathering processes. *Earth Surface Processes and Landforms*, **32**, 888–904.

Parchure, T.M. and Mehta, A.J. 1985. Erosion of soft cohesive sediment deposits. *Journal of the Hydraulics Division, American Society of Civil Engineers* **111**, 1308–1326.

Parker, G.G., Sr., Higgins, C.G. and Wood, W.W. 1990, Piping and pseudokarst in drylands. *Geological Society of America Special Paper* **252**, 77–110.

Parsons, A.J., Wainwright, J. and Abrahams, A.D. 1996. Runoff and erosion on semi-arid hillslopes, In *Advances in Hillslope Processes*, Anderson, M. G. and Brooks, S.M. (eds), 1061–1078. Chichester: John Wiley & Sons.

Parthenaides, E. 1965. Erosion and deposition of cohesive soils. *Journal of the Hydraulics Division, American Society of Civil Engineers* **91**, 105–139.

Parthenaides, E. and Paaswell, R.R. 1970. Erodibility of channels with cohesive banks. Journal of the Hydraulics Division, *American Society of Civil Engineers* **96**, 755–771.

Patton, P.C. and Schumm, S.A., 1975. Gully erosion, Northwestern Colorado; A threshold phenomenon. *Geology* **3**, 88–89.

Pavich, M.J., 1989. Regolith residence time and the concept of surface age of the Piedmont "peneplain". *Geomorphology* **2**, 181–196.

Poesen, J. and Govers, G. 1990. Gully erosion in the loam belt of Belgium: typology and control measures. In *Soil Erosion on Agricultural Land*, Boardman, J., Foster, I.D.L. and Dearing, J.A., (eds), 513–530. Chichester: John Wiley & Sons.

Poesen, J., Nachtergaele, J., Verstraeten, G. and Valentin, C. 2003. Gully erosion and environmental change: importance and research needs. *Catena* **50**, 91–133.

Poesen, J., Vanwalleghem, T., de Venta, J., Verstraeten, G. and Martínez-Casasnovak, J.A. 2006. Gully erosion in Europe. In *Soil Erosion in Europe*, Boardman, J. and Poesen, J. (eds), 515–536. Chichester: Wiley.

Prosser, I.P. and Abernethy, B. 1996. Predicting the topographic limits to a gully network using a digital terrain model and process thresholds. *Water Resources Research* **32**, 2289–2298.

Prosser, I.P., Chappell, J. and Gillespie, R. 1994. Holocene valley aggradation and gully erosion in headwater catchments, southeastern highlands of Australia. *Earth Surface Processes and Landforms* **19**, 465–480.

Prosser, I.P. and Dietrich, W.E. 1995. Field experiments on erosion by overland flow and their implication for a digital terrain model of channel initiation. *Water Resources Research* **31**, 2867–2876.

Prosser, I.P., Dietrich, W.E. and Stevenson, J. 1995. Flow resistance and sediment transport by concentrated overland flow in a grassland valley. *Geomorphology* **13**, 71–86.

Prosser, I.P. and Slade, C.J. 1994. Gully formation and the role of valley-floor vegetation, southeastern Australia. *Geology* **22**, 1127–1130.

Rauws, G. 1987. The initiation of rills on plane beds of non-cohesive sediments. *Catena Supplement* **8**, 107–118.

Rauws, G. and Govers, G. 1988. Hydraulic and soil mechanical aspects of rill generation on agricultural soils. *Journal of Soil Science* **39**, 111–124.

Reid, L.M. 1989. Channel formation by surface runoff in grassland catchments, unpublished Ph.D. thesis, University of Washington, Seattle, 139pp.

Reneau, S.L. and Dietrich, W.E. 1991. Erosion rates in the southern Oregon Coast range: evidence for an equilibrium between hillslope erosion and sediment yield, *Earth Surface Processes And Landforms* **16**, 307–322.

Robinson, K.M. and Hanson, G.J. 1994. A deterministic headcut advance model. *Transactions American Society of Agriculture Engineers* **37**, 1437–1443.

Robinson, K.M. and Hanson, G.J. 1995. Large-scale headcut erosion testing. *Transactions American Society of Agricultural Engineers* **38**, 429–434.

Roering, J.J., Kirchner, J.W. and Dietrich, W.E. 1999. Evidence for nonlinear, diffusive sediment transport on hillslopes and implications for landscape morphology. *Water Resources Research* **35**, 853–870.

Roering, J.J., Kirchner, J.W. and Dietrich, W.E. 2001a. Hillslope evolution by nonlinear, slope-dependent transport; steady state morphology and equilibrium adjustment timescales. *Journal of Geophysical Research* **106**, 16,499–16,513.

Roering, J.J., Kirchner, J.W., Sklar, L.S. and Dietrich, W.E. 2001b. Hillslope evolution by nonlinear creep and landsliding: An experimental study. *Geology* **29**, 143–146.

Rutherford, I.D., Prosser, I.P. and Davis, J. 1997. Simple approaches to predicting rates of gully development. In *Management of Landscapes Disturbed by Channel Incision*, Wang, S.Y., Langendoen, E.J. and Shields, F.D. Jr. (eds.), 1125–1130. Oxford, Miss: University of Mississippi.

Savat, J. 1976. Discharge velocities and total erosion of a calcareous loess: a comparison between pluvial and terminal runoff. *Revue Geomorphologie Dynamique* **24**, 113–122.

Savat, J. 1980. Resistance to flow in rough supercritical sheetflow. *Earth Surface Processes* **5**, 103–122.

Savat, J. 1982. Common and uncommon selectivity in the process of fluid transportation: field observations and laboratory experiments on bare surfaces. *Catena Supplement* **1**, 139–160.

Savat, J. and De Ploey, J. 1982. Sheetwash and rill development by surface flow. In *Badland Geomorphology and Piping*, Bryan, R. and Yair, A. (eds), 113–125. Norwich: Geo Books.

Schumm, S.A. 1956a. Evolution of drainage systems and slopes in badlands at Perth Amboy, New Jersey. *Geological Society of America Bulletin* **67**, 597–646.

Schumm, S.A. 1956b. The role of creep and rainwash on the retreat of badland slopes. *American Journal of Science* **254**, 693–706.

Schumm, S.A. 1962. Erosion on miniature pediments in Badlands National Monument, South Dakota. *Geological Society of America Bulletin* **73**, 719–724.

Schumm, S.A. 1963. Rates of surficial rock creep on hillslopes in western Colorado. *Science* **155**, 560–561.

Schumm, S.A. 1964. Seasonal variations of erosion rates and processes on hillslopes in western Colorado. *Zeitschrift für Geomorphologie Supplementband* **5**, 215–238.

Schumm, S.A. and Hadley, R.F. 1957. Arroyos and the semiarid cycle of erosion. *American Journal of Science* **255**, 164–174.

Schumm, S.A., Harvey, M.D. and Watson, C.C. 1984. *Incised Channels; Morphology, Dynamics and Control*. Littleton, Co: Water Resources Publications, 200pp.

Schumm, S.A. and Lusby, G.C. 1963. Seasonal variation of infiltration capacity and runoff on hillslopes in western Colorado. *Journal of Geophysical Research* **68**, 3655–3666.

Sidorchuk, A. 2005. Stochastic components in the gully erosion modelling. *Catena* **63**, 299–317.

Slaymaker, O. 1982. The occurrence of piping and gullying in the Penticton glacio-lacustrine silts, Okanagan Valley, B.C. In *Badland Geomorphology and Piping*, Bryan, R.B. and Yair, A. (eds), 305–316. Norwich: GeoBooks.

Smith, K.G. 1958. Erosional processes and landforms in Badlands National Monument, South Dakota. *Bulletin of the Geological Society of America* **69**, 975–1008.

Smith, T.R. and Bretherton, F.P. 1972. Stability and the conservation of mass in drainage basin evolution. *Water Resources Research* **8**, 1506–1529.

Stein, O.R. and Julien, P.Y. 1993. A criterion delineating the mode of headcut migration. *American Society Civil Engineers, Journal of the Hydraulics Division* **119**, 37–50.

Stein, O.R., Julien, P.J. and Alonso, C.V. 1997. Headward advancement of incised channels. In *Management of Landscapes Disturbed by Channel Incision*, Wang, S.Y. Langendoen, E.J. and Shields, F.D. Jr., 497–503. Oxford, Mississippi: University of Mississippi.

Thornes, J.B. 1985. The ecology of erosion. *Geography* **70**, 222–236.

Torri, D. and Borselli, L. 2003. Equation for high-rate gully erosion. *Catena* **50**, 449–467.

Torri, D., Sfalanga, M. and Chisci, G. 1987. Threshold conditions for incipient rilling. *Catena Supplement* **8**, 97–115.

Trimble, S.W. 1974. *Man-Induced Soil Erosion on the Southern Piedmont, 1700–1970*, Soil Conservation Society, Ankemy, Iowa, 180pp.

Tucker, G.E. 2004. Drainage basin sensitivity to tectonic and climatic forcing; implications of a stochastic model for the role of entrainment and erosion thresholds. *Earth Surface Processes and Landforms* **29**, 185–205.

Tucker, G.E. and Bras, R.L. 1998. Hillslope processes, drainage density, and landscape morphology. *Water Resources Research* **34**, 2751–2764.

Tucker, G.E. Arnold, J.R., Bras, R.L., Flores, H., Istanbulloglu, E. and Sólyom, P. 2006. Headwater channel dynamics in semiarid rangelands, Colorado high plains, USA. *Bulletin of the Geological Society of America* **118**, 959–974.

Tucker, G.E. and Slingerland, R. 1997. Drainage basin responses to climate change. *Water Resources Research* **33**, 2031–2047.

Valentin, C., Poesen, J. and Li, Y. 2005. Gully erosion: Impacts, factors and control. *Catena* **63**, 132–153.

Vandaele, K., Poesen, J., Govers, G. and van Wesemael, B. 1996. Geomorphic threshold conditions for ephemeral gully incision. *Geomorphology* **16**, 161–173.

Vandekerckhove, L., Poesen, J., Wijdenes, D.O. and de Figueiredo, T. 1998. Topographical thresholds for ephemeral gully initiation in intensively cultivated areas of the Mediterranean. *Catena* **33**, 271–292.

Vice, R.B., Guy, H.P. and Ferguson, G.E. 1968. Sediment movement in an area of suburban highway construction – Scott Run Basin, Virginia – 1961–64. *U.S. Geology Survey Water-Supply Paper* **1591-E**, 41pp.

Wang, S.S.Y., Langendoen, E.J. and Shields, F.D.J. (eds.). 1997. *Management of Landscapes Disturbed by Channel Incision: Stabilization, Rehabilitation, Restoration*. Center for Computational Hydroscience and Engineering, University of Mississippi, University, Mississippi, 1134pp.

Wells, S.G. and Gutierrez, A.A. 1982. Quaternary evolution of badlands in the southeastern Colorado Plateau, U.S.A. In*Badland Geomorphology and Piping*, R. Bryan and A. Yair (eds), 239–257. Norwich: Geo Books.

Willgoose, G. 2005. Mathematical modeling of whole landscape evolution. *Annual Review of Earth and Planetary Sciences* **33**, 443–459.

Williams, J.R., Jones, C.A. and Dyke, P.T. 1984. A modeling approach to determining the relationship between erosion and soil productivity. *Transactions of the American Society of Civil Engineers* **27**, 129–144.

Wolman, M.G. 1967. A cycle of sedimentation and erosion in urban river channels. *Geografiska Annaler* **49A**, 385–395.

Woodward, D.E. 1999. Method to predict cropland ephemeral gully erosion. *Catena* **37**, 393–399.

Yair, A., Lavee, H., Bryan, R.B. and Adar, E. 1980. Runoff and erosion processes and rates in the Zin Valley badlands, northern Negev, Israel. *Earth Surface Processes* **5**, 205–225.

Zhu Xianmo (ed.), 1986. *Land Resources on the Loess Plateau of China*, Northwest Inst. Soil and Water Conservation., Academia Sinica, Shaanxi Science and Technique Press.